SIAM J. SCI. COMPUT.
Vol. 38, No. 5, pp. A3318–A3356



# OPTIMAL LOCAL APPROXIMATION SPACES FOR COMPONENT-BASED STATIC CONDENSATION PROCEDURES*

KATHRIN SMETANA† AND ANTHONY T. PATERA†

**Abstract.** In this paper we introduce local approximation spaces for component-based static condensation (sc) procedures that are optimal in the sense of Kolmogorov. To facilitate simulations for large structures such as aircraft or ships, it is crucial to decrease the number of degrees of freedom on the interfaces, or "ports," in order to reduce the size of the statically condensed system. To derive optimal port spaces we consider a (compact) transfer operator that acts on the space of harmonic extensions on a two-component system and maps the traces on the ports that lie on the boundary of these components to the trace of the shared port. Solving the eigenproblem for the composition of the transfer operator and its adjoint yields the optimal space. For a related work in the context of the generalized finite element method, we refer the reader to [I. Babuška and R. Lipton, *Multiscale Model. Simul.*, 9 (2011), pp. 373–406]. We further introduce a spectral greedy algorithm to generalize the procedure to the parameter-dependent setting and to construct a quasi-optimal parameter-independent port space. Moreover, it is shown that, given a certain tolerance and an upper bound for the ports in the system, the spectral greedy constructs a port space that yields an sc approximation error on a system of arbitrary configuration which is smaller than this tolerance for all parameters in a rich train set. We present our approach for isotropic linear elasticity, although the idea may be readily applied to any linear coercive problem. Numerical experiments demonstrate the very rapid and exponential convergence both of the eigenvalues and of the sc approximation based on spectral modes for nonseparable and irregular geometries such as an I-beam with an internal crack.

**Key words.** domain decomposition methods, (component-based) static condensation, model reduction, component mode synthesis, a priori error estimate, Kolmogorov $n$-width, finite element method, reduced basis methods

**AMS subject classifications.** 65N12, 65N55, 65N15, 65N30, 74S05

**DOI.** 10.1137/15M1009603

## 1. Introduction.

In the last decades numerical simulations based on partial differential equations (PDEs) have significantly gained importance in engineering applications. However, both the geometric complexity of the considered structures, such as ships, aircraft, and turbines, and the intricacy of the simulated physical phenomena often make a straightforward application of, say, the finite element (FE) method prohibitive. This is particularly true if multiple simulation requests or a real-time simulation response is desired, as in engineering design and optimization.

One way to tackle such complex problems is to exploit the natural decomposition of the structures into components and apply static condensation (sc) to obtain a (Schur complement) system of the size of the degrees of freedom (DOFs) on all interfaces or ports in the system. To mitigate the computational costs for the required PDE solvers in the interior of the component, model order reduction procedures may be applied. One popular approach is component mode synthesis (CMS), introduced in [4, 21], which uses an approximation based on the eigenmodes of local constrained eigenvalue problems. The static condensation reduced basis element (scRBE) method [22, 23]

*Submitted to the journal's Methods and Algorithms for Scientific Computing section February 23, 2015; accepted for publication (in revised form) July 28, 2016; published electronically October 19, 2016.

http://www.siam.org/journals/sisc/38-5/M100960.html

**Funding:** This work was supported by OSD/AFOSR/MURI grant FA9550-09-1-0613 and ONR grant N00014-11-1-0713.

†Department of Mechanical Engineering, Massachusetts Institute of Technology, Cambridge, MA 02139 (ksmetana@mit.edu, patera@mit.edu).

has been introduced in the context of parametrized PDEs and employs the reduced basis (RB) method [15, 17, 38] for the approximation in the interior of the component, benefiting from the, in general, very rapid convergence of RB approximations [5, 7, 9]. The scRBE method allows an offline/online decomposition in the sense that high-dimensional computations that are necessary to construct the reduced model are carried out in a (possibly expensive) offline phase, such that in the online stage only computations that scale with the DOFs on the ports must be performed.

To realize a fast simulation response also for large component-based structures it is vital to reduce the number of DOFs on the ports, too. Within the CMS approach this is realized by utilizing an eigenmode expansion [6, 18, 19, 26], which has recently been combined with input-output-based model reduction in [20]. In [11] Eftang and Patera develop an empirical pairwise training procedure for port reduction within the scRBE context: Modes are selected from traces of snapshots generated by random boundary conditions.

In this paper we propose port spaces for component-based sc procedures that are optimal in the sense of Kolmogorov [29] and thus minimize the sc approximation error among all spaces that have the same dimension. In constructing those port spaces we are guided by the goal to provide a (quasi-)optimal space for the global system. In detail, we connect two components[1] at the port for which we wish to construct the port space and recognize that the solution on the global system satisfies the PDE locally with unknown Dirichlet boundary conditions on the ports that lie on the boundary of the two-component system. Therefore, we consider the space of all harmonic extensions on this local system, i.e., all local solutions of the PDE. Note that from separation of variables we anticipate an exponential decay (of the higher modes) of the Dirichlet boundary conditions to the interior of the system; thus, most of the harmonic extensions have very small values on the shared port, which is why we expect that a low-dimensional port space will yield already a very good approximation of all harmonic extensions. To quantify which information of the Dirichlet boundary conditions reaches the shared port of the system, we introduce a (compact) transfer operator that acts on the space of harmonic extensions and maps the traces (of the harmonic extensions) on the boundary ports to the trace on the shared port. Solving the "transfer eigenproblem" for the composition of the transfer operator and its adjoint yields the optimal space. We note that a similar eigenproblem has been considered in the work of Babuška and Lipton (see [2, 3]) for the generalized FE method.

We can also view our method as a more formal approach to the transfer matrix method (see, for instance, [36]), in which the transfer of the field both between components and within components are taken into account to obtain a frequency equation for a system of components. The necessary relations are derived, for instance, from equilibrium equations.

To construct a (quasi-)optimal port space in the parametrized setting we also introduce a spectral greedy algorithm that constructs a parameter-independent port space, which serves to approximate all parameter-dependent port spaces obtained from the now parameter-dependent transfer eigenproblem. First, we exploit an a priori bound, which is also derived in this article, to construct parameter-dependent port spaces such that the sc approximation based on the respective parameter-dependent

[1] Note that one could also connect more components to construct port spaces for several ports at once. However, in order to realize an efficient computational realization and make use of parallelization concepts, considering two components is often preferable.

port space lies below a given tolerance. In the spirit of the greedy algorithm for RB methods introduced in [44], the spectral greedy then proceeds iteratively and identifies at each iteration the function in the union of all parameter-dependent port spaces which is worst approximated by the current space. The spectral greedy algorithm provides a reduced basis for the approximation of the $n$ eigenspaces associated with the $n$ largest eigenvalues of a parametrized (generalized) eigenproblem with a given accuracy for $n > 1$. Note that the spectral greedy algorithm also shares some similarities with the POD-greedy algorithm [14, 16], as each parameter is associated with a space and not a single function, as in the "standard" greedy. Finally, given an upper bound for the anticipated number of ports in the online system, the spectral greedy algorithm constructs a port space such that the sc approximation error in the online stage is bounded (for all parameters in a rich train set) by a prescribed tolerance. In this sense, we ensure convergence of the sc approximation.

We emphasize that, in contrast to existing approaches, the port spaces generated by our approach both allow for a rigorous a priori theory and yield a rapidly (and often exponentially) convergent sc approximation, as demonstrated in the numerical experiments. The eigenmode expansion employed in the CMS approach also admits a rigorous a priori theory, but provides only an algebraic convergence rate. Conversely, empirical approaches often realize a rapid convergent sc approximation; however, there do not exist either a priori error bounds or algorithms to construct a port space of specified accuracy.

There are various other approaches that are based on localized approximation spaces for parametrized PDEs as, for instance, in the context of multiscale methods [1, 10, 35, 40]. A combination of domain decomposition (DD) and RB methods was first considered in the reduced basis element method (RBEM) [31, 32], where the local RB approximations are coupled by Lagrange multipliers. The RB hybrid method [24] extends the RBEM by additionally considering a coarse FE discretization on the whole domain to account for continuity of normal stresses. In the RDF method, FE basis functions on the interface or on a (small) area around the interface are combined with local RB approximations that are harmonic extensions of either parametrized Lagrangian or Fourier functions [25]. Finally, RB methods have been combined with a Dirichlet–Neumann scheme in [33] and with a heterogeneous DD method in [34], where the basis on the interface in the latter article is constructed from snapshots. We believe that our approach might be relevant to many of these DD model reduction techniques.

The remainder of this paper is organized as follows. In section 2 we give a short introduction to DD methods and recall the port-reduced sc procedure. The main new contributions of this paper are developed in sections 3 and 4. In the former we first introduce optimal port spaces and prove an a priori bound for the corresponding sc approximation still in the parameter-free setting. Subsequently, we address in section 4 parametrized PDEs and introduce an algorithm to construct a parameter-independent port space and prove convergence for the resulting parameter-dependent sc approximation. The results in sections 3 and 4 are derived for a two-component system, as all relevant ideas of our approach can be explained in this simple setting. The generalization to arbitrary systems is discussed in section 5. Finally, we present several numerical experiments in section 6 to validate the approximation properties of our approach, and in section 7 we draw some conclusions. We emphasize that in order to simplify the presentation we present our approach for isotropic linear elasticity; however, all results hold true for coercive, linear PDEs, whose associated bilinear form is symmetric.

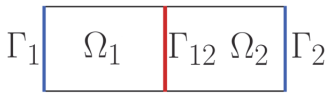


FIG. 2.1. *Illustration of the decomposition of $\Omega$ in $\Omega_1$ and $\Omega_2$ and the position of the ports $\Gamma_1, \Gamma_{12}, \Gamma_2$ within $\Omega$ in a simplified two-dimensional setting.*

**2. Preliminaries.** Let $\widehat{\Omega} \subset \mathbb{R}^3$ be a large, bounded domain. In sections 3 and 4 we will demonstrate how to obtain an optimal local approximation space on a subdomain $\Omega \subset \widehat{\Omega}$, and we discuss in section 5 how these optimal local spaces can be employed to obtain a quasi-optimal space for the entire domain $\widehat{\Omega}$.

Let $n$ be the outer normal of $\Omega$, and let the Lipschitz boundary $\partial\Omega$ be partitioned such that $\partial\bar{\Omega} = \bar{\Sigma}_D \cup \bar{\Sigma}_N$, with $|\Sigma_D| > 0$. We assume that $\Omega$ represents an isotropic material, and we consider the following linear elastic boundary value problem: Find the displacement vector $u$ and the Cauchy stress tensor $\sigma(u)$ such that

$$-\nabla \cdot \sigma(u) = \mathbf{g} \quad \text{in } \Omega, \qquad \sigma(u) \cdot n = 0 \quad \text{on } \Sigma_N, \qquad u = u_D \quad \text{on } \Sigma_D, \tag{2.1}$$

where $\mathbf{g} = (g^1, g^2, g^3) \in \mathbb{R}^3$ is a body force and accounts for gravity. Moreover, $u_D$ is the *unknown* value of the global solution corresponding to $\widehat{\Omega}$ on $\Sigma_D$ and therefore an (unknown) Dirichlet boundary condition on the displacement over $\Omega$. We can express for a linear elastic material the Cauchy stress tensor as $\sigma(u) = E\,C : \varepsilon(u)$, where $C$ is the fourth-order stiffness tensor, $\varepsilon(u) = 0.5(\nabla u + (\nabla u)^T)$ is the infinitesimal strain tensor, and the colon operator : is defined as $C : \varepsilon(u) = \sum_{k,l=1}^{3} C_{ijkl}\varepsilon_{kl}(u)$. Moreover, $E \in L^\infty(\Omega)$ denotes Young's modulus, which is assumed to be piecewise constant on $\Omega$ and to satisfy $E(x) \geq E_0 > 0$ for a constant $E_0 \in \mathbb{R}^+$. Therefore, the stiffness tensor can be written as

$$C_{ijkl} = \frac{\nu}{(1+\nu)(1-2\nu)}\delta_{ij}\delta_{kl} + \frac{1}{2(1+\nu)}(\delta_{ik}\delta_{jl} + \delta_{il}\delta_{jk}), \quad 1 \leq i,j,k,l \leq 3, \tag{2.2}$$

where $\delta_{ij}$ denotes the Kronecker delta; we choose Poisson's ratio $\nu = 0.3$. The corresponding variational formulation of (2.1) then reads as follows: Find $u \in X = \{v \in [H^1(\Omega)]^3 \ : \ v = u_D \text{ on } \Sigma_D\}$ such that

$$a(u,v) = f(v) \quad \forall v \in X_0, \quad \text{where } X_0 := \{v \in [H^1(\Omega)]^3 \ : \ v = 0 \text{ on } \Sigma_D\}, \tag{2.3}$$

and the bilinear and linear forms $a(\cdot,\cdot) : [H^1(\Omega)]^3 \times [H^1(\Omega)]^3 \to \mathbb{R}$ and $f(\cdot) : [H^1(\Omega)]^3 \to \mathbb{R}$ are defined as

$$a(w,v) := \int_\Omega E(x)\,\frac{\partial w^i}{\partial x_j} C_{ijkl}\,\frac{\partial v^k}{\partial x_l}\,dx \quad \text{and} \quad f(v) := \int_\Omega \mathbf{g}\cdot v\,dx. \tag{2.4}$$

Well-posedness of (2.3) follows then from Korn's inequality, treating the nonhomogeneous Dirichlet boundary conditions with the standard lifting procedure.

**2.1. The multidomain problem.** For the sake of simplicity we decompose $\Omega$ into two nonoverlapping subdomains (components) such that

$$\bar{\Omega} = \bar{\Omega}_1 \cup \bar{\Omega}_2, \tag{2.5}$$

as illustrated in Figure 2.1 in a simplified two-dimensional setting. We denote by $\Gamma_{12}$ the interface between $\Omega_1$ and $\Omega_2$:

$$\Gamma_{12} = \bar{\Omega}_1 \cap \bar{\Omega}_2. \tag{2.6}$$

For the sake of simplicity we assume that each component has two local interfaces (ports) at which this component may be connected to other components. Moreover, we assume that those ports do not intersect. The nonshared port of component $i$ is denoted by $\Gamma_i$, $i = 1, 2$, and we require $\bar{\Sigma}_D = \bar{\Gamma}_1 \cup \bar{\Gamma}_2$, which implies $\Gamma_{12} \cap \Sigma_D = \emptyset$. We emphasize that the generalization to the case where the ports are not necessarily mutually disjoint is not straightforward and thus the subject of future work. Subdomains which have more than two interfaces are discussed in section 5.

To obtain a variational formulation of the multidomain problem, we introduce the local spaces $X_i = \{v \in [H^1(\Omega_i)]^3 : v|_{\Gamma_i} = u_D|_{\Gamma_i}\}$ and $X_{i;0} := \{v \in X_i : v|_{\Gamma_i} = v|_{\Gamma_{12}} = 0\}$, $i = 1, 2$, and define the following linear and bilinear forms:

(2.7)
$$a_i(w, v) := \int_{\Omega_i} E(x) \frac{\partial w^i}{\partial x_j} C_{ijkl} \frac{\partial v^k}{\partial x_l} dx, \quad f_i(v) := \int_{\Omega_i} \mathbf{g} \cdot v \, dx \quad \forall w, v \in [H^1(\Omega_i)]^3.$$

Then the variational formulation of (2.1) can equivalently be stated in the following way (see, for instance, [39]): Find $u_1 \in X_1$ and $u_2 \in X_2$ such that

$$a_1(u_1, v) = f_1(v) \qquad \forall v \in X_{1;0}, \tag{2.8a}$$
$$a_2(u_2, v) = f_2(v) \qquad \forall v \in X_{2;0}, \tag{2.8b}$$
$$u_1 = u_2 \qquad \text{on } \Gamma_{12}, \tag{2.8c}$$
$$a_1(u_1, \mathcal{R}_1\zeta) + a_2(u_2, \mathcal{R}_2\zeta) = f_1(\mathcal{R}_1\zeta) + f_2(\mathcal{R}_2\zeta) \quad \forall \zeta \in [H^{1/2}(\Gamma_{12})]^3, \tag{2.8d}$$

where $\mathcal{R}_i : [H^{1/2}(\Gamma_{12})]^3 \to X_i^{\Gamma_i} := \{v \in [H^1(\Omega_i)]^3 : v|_{\Gamma_i} = 0\}$ are linear and continuous extension operators. Note that if we knew the value of $u$ on $\Gamma_{12}$, we could determine $u$ on the whole computational domain $\Omega$ thanks to (2.8a) and (2.8b).

Finally, we define local semi-inner products and seminorms $(v, w)_{X_i} := a_i(v, w)$ and $\|v\|_{X_i} := \sqrt{(v, v)_{X_i}}$ for all $v, w \in [H^1(\Omega_i)]^3$, $i = 1, 2$, and the corresponding global (semi-)inner product and (semi)norm $(v, w)_X := \sum_{i=1}^2 (v, w)_{X_i}$ and $\|v\|_X := (\sum_{i=1}^2 \|v\|_{X_i}^2)^{1/2}$.

**2.2. (Port-reduced) static condensation.** The variational formulation (2.8) is at the basis of many DD methods, such as iterative substructuring methods (see, for instance, [39] for an overview). The key concept of static condensation procedures is to first employ (2.8) to derive an equation for $u|_{\Gamma_{12}} \in [H^{1/2}(\Gamma_{12})]^3$ and then discretize this equation in order to compute an approximation for $u|_{\Gamma_{12}}$ and thus for $u$.

To derive a well-posed problem for $u|_{\Gamma_{12}} \in [H^{1/2}(\Gamma_{12})]^3$, we first note that the solutions $u_i \in X_i$ of (2.8) can be written as a sum of an $a$-harmonic extension of the nonhomogeneous Dirichlet boundary conditions, an $a$-harmonic extension of the unknown vector $u|_{\Gamma_{12}}$, and a Riesz representation of the right-hand side; to wit, there holds[2]

$$u_i = \mathcal{L}_{i,\Gamma_i} u_{D,i} + \mathcal{L}_{i,\Gamma_{12}}(u|_{\Gamma_{12}}) + b_i^f. \tag{2.9}$$

Here, the $a$-harmonic extension operators $\mathcal{L}_{i,\Gamma} : [H^{1/2}(\Gamma)]^3 \to [H^1(\Omega_i)]^3$, $i = 1, 2$, are defined as

$$a_i(\mathcal{L}_{i,\Gamma}\zeta, v) = 0 \quad \forall v \in X_{i;0} \text{ and } (\mathcal{L}_{i,\Gamma}\zeta)|_\Gamma = \zeta, \quad (\mathcal{L}_{i,\Gamma}\zeta)|_{\Gamma^*} = 0, \ \Gamma \neq \Gamma^*, \tag{2.10}$$

[2]Note that in actual practice one would use arbitrary continuous extensions of the nonhomogeneous Dirichlet boundary conditions and associated solutions of the PDE with these extensions as a right-hand side.

for any $\zeta \in [H^{1/2}(\Gamma)]^3$, $\Gamma = \Gamma_1, \Gamma_{12}, \Gamma_2$, $u_{D,i} := u_D|_{\Gamma_i} \in [H^{1/2}(\Gamma_i)]^3$, and the Riesz representations $b_i^f \in X_{i;0}$ of the right-hand side are defined as the solutions of

$$a_i(b_i^f, v) = f_i(v) \quad \forall v \in X_{i;0}, \ \ i = 1, 2. \tag{2.11}$$

To shorten notation we set $b^f := b_1^f + b_2^f$, extending $b_i^f$ by zero to $\Omega_{i'}$, $i \neq i'$.

Inserting (2.9) into (2.8d) and exploiting that the operators $\mathcal{L}_{i,\Gamma}$, $\Gamma = \Gamma_1, \Gamma_{12}, \Gamma_2$ are continuous extension operators (cf. [30]), we obtain the variational form of the Steklov–Poincaré interface equation: Find $u|_{\Gamma_{12}} \in [H^{1/2}(\Gamma_{12})]^3$ such that

$$\sum_{i=1}^{2} a_i(\mathcal{L}_{i,\Gamma_{12}}(u|_{\Gamma_{12}}), \mathcal{L}_{i,\Gamma_{12}}\zeta) = \sum_{i=1}^{2} \left[ f_i(\mathcal{L}_{i,\Gamma_{12}}\zeta) - a_i(b_i^f, \mathcal{L}_{i,\Gamma_{12}}\zeta) - a_i(\mathcal{L}_{i,\Gamma_i} u_{D,i}, \mathcal{L}_{i,\Gamma_{12}}\zeta) \right], \tag{2.12}$$

for all $\zeta \in [H^{1/2}(\Gamma_{12})]^3$. Note that well-posedness of problem (2.12) can, for instance, be demonstrated by using the Riesz representation theorem and exploiting that the bilinear forms $(\cdot,\cdot)_\Gamma : [H^{1/2}(\Gamma)]^3 \times [H^{1/2}(\Gamma)]^3 \to \mathbb{R}$ on the ports $\Gamma = \Gamma_1, \Gamma_{12}, \Gamma_2$ and the union of ports $\Gamma = \Gamma_1 \cup \Gamma_2$, defined as

$$\begin{aligned} (\zeta, \rho)_{\Gamma_{12}} &:= \sum_{i=1}^{2} a_i(\mathcal{L}_{i,\Gamma_{12}}\zeta, \mathcal{L}_{i,\Gamma_{12}}\rho), \\ (\zeta, \rho)_{\Gamma_i} &:= a_i(\mathcal{L}_{i,\Gamma_i}\zeta, \mathcal{L}_{i,\Gamma_i}\rho), \ \ i = 1, 2, \ \text{ and } \ (\zeta, \rho)_{\Gamma_1 \cup \Gamma_2} := (\zeta, \rho)_{\Gamma_1} + (\zeta, \rho)_{\Gamma_2}, \end{aligned} \tag{2.13}$$

are inner products. Here, the positive definiteness of $(\cdot,\cdot)_\Gamma$ follows from Friedrich's inequality, Korn's inequality, and the trace theorem. Furthermore, we introduce for all $v \in [H^{1/2}(\Gamma)]^3$ the induced norm $\|v\|_\Gamma := \sqrt{(v,v)_\Gamma}$, $\Gamma = \Gamma_1, \Gamma_{12}, \Gamma_2, \Gamma_1 \cup \Gamma_2$.

In order to compute an approximation of $u|_{\Gamma_{12}} \in [H^{1/2}(\Gamma_{12})]^3$ we introduce a basis $\{\chi_k\}_{k=1}^{\infty}$ of $[H^{1/2}(\Gamma_{12})]^3$. At this point we assume that this basis is given to us, where the choice of the basis is addressed in the next section. Moreover, we introduce the functions

$$\Phi_k := \begin{cases} \mathcal{L}_{1,\Gamma_{12}}\chi_k & \text{in } \Omega_1, \\ \mathcal{L}_{2,\Gamma_{12}}\chi_k & \text{in } \Omega_2, \end{cases} \tag{2.14}$$

the space of interface functions

$$X_{\Gamma_{12}} := \operatorname{span}\{\Phi_k, \ \ k = 1, \ldots, \infty\},$$

and a reduced space

$$X_{\Gamma_{12}}^m := \operatorname{span}\{\Phi_k, \ \ k = 1, \ldots, m\}.$$

We may then introduce a port-reduced static condensation approximation [11]

$$u^m = \sum_{i=1}^{2} \left(b_i^f + \mathcal{L}_{i,\Gamma_i} u_{D,i}\right) + \sum_{k=1}^{m} U_k^m \Phi_k, \quad m \leq \infty, \tag{2.15}$$

where the coefficients $U_k^m \in \mathbb{R}$ are the solutions of the Schur complement system

$$\sum_{k=1}^{m} a(U_k^m \Phi_k, \Phi_l) = f(\Phi_l) - a(b^f, \Phi_l) - \sum_{i=1}^{2} a_i(\mathcal{L}_{i,\Gamma_i} u_{D,i}, \Phi_l), \quad l = 1, \ldots, m. \tag{2.16}$$

Well-posedness of (2.16) follows from the Lax–Milgram lemma. Note that the solution $u$ of (2.3) can be represented as in (2.15) with $m = \infty$ and solves (2.16) for the test space $X_{\Gamma_{12}}$. Moreover, thanks to the definition of $\Phi_k$ in (2.14), the system (2.16) for $m = \infty$ is just a reformulation of (2.12).

We may now ask how to find a rapidly convergent or even optimal $m$-dimensional port space $\Lambda^m = \text{span}\{\chi_k\}_{i=1}^m \subset [H^{1/2}(\Gamma_{12})]^3$, and thus local approximation space $X^m_{\Gamma_{12}}$, for all solutions $u$ of (2.3) for all possible Dirichlet boundary data $u_{D,i} \in [H^{1/2}(\Gamma_i)]^3$, $i = 1, 2$. This question will be addressed in the next section.

**3. Optimal port spaces.** Recall that we have assumed that $\Omega$ lies in the interior of a large computational domain $\widehat{\Omega}$ such that we do not know the values of $u$ on $\Gamma_1$ and $\Gamma_2$. We know only that $u$ must solve the PDE (2.3) locally on $\Omega$—with unknown Dirichlet boundary conditions $u_D$. The goal of this section is thus to construct a port space which can provide a rapidly convergent approximation to the set of all (local) solutions $u$ of (2.3) on $\Omega$. Aiming at finding a good approximation space for a whole set of functions suggests optimality in the sense of Kolmogorov [29].

DEFINITION 3.1. *Let $\Lambda$ be a Hilbert space, let $A \subset \Lambda$, and let $\Lambda^n$ be an $n$-dimensional subspace of $\Lambda$. The deviation of $A$ from $\Lambda^n$ is*[3]

$$E(A; \Lambda^n) := \sup_{\xi \in A} \inf_{\zeta \in \Lambda^n} \|\xi - \zeta\|_\Lambda. \tag{3.1}$$

*The Kolmogorov $n$-width of $A$ in $\Lambda$ is given by*

$$\begin{aligned} d_n(A; \Lambda) &:= \inf\{E(A; \Lambda^n) \,:\, \Lambda^n \text{ an } n\text{-dimensional subspace of } \Lambda\} \\ &= \inf_{\substack{\Lambda^n \subset \Lambda \\ \dim(\Lambda^n) = n}} \sup_{\xi \in A} \inf_{\zeta \in \Lambda^n} \|\xi - \zeta\|_\Lambda. \end{aligned} \tag{3.2}$$

*Moreover, for linear, continuous operators $T : Y \to \Lambda$ and a Hilbert space $Y$ we also introduce*

(3.3)

$$d_n(T(Y); \Lambda) := \inf_{\substack{\Lambda^n \subset \Lambda \\ \dim(\Lambda^n) = n}} \sup_{\psi \in Y} \inf_{\zeta \in \Lambda^n} \frac{\|T\psi - \zeta\|_\Lambda}{\|\psi\|_Y} = \inf_{\substack{\Lambda^n \subset \Lambda \\ \dim(\Lambda^n) = n}} \sup_{\|\psi\|_Y \le 1} \inf_{\zeta \in \Lambda^n} \|T\psi - \zeta\|_\Lambda.$$

*A subspace $\Lambda^n \subset \Lambda$ of dimension at most $n$ for which*

$$d_n(A; \Lambda) = E(A; \Lambda^n) \quad \text{or} \quad d_n(T(Y); \Lambda) = \sup_{\psi \in Y} \inf_{\zeta \in \Lambda^n} \frac{\|T\psi - \zeta\|_\Lambda}{\|\psi\|_Y}$$

*holds is called an optimal subspace for $d_n(A; \Lambda)$ or $d_n(T(Y); \Lambda)$, respectively.*

*Remark* 3.2. Note that the definition of $d_n(T(Y); \Lambda)$ is related to the definition of $d_n(A; \Lambda)$ in the sense that in the former we consider the subset $T(Y) \subset \Lambda$, which is characterized by the image of the mapping $T$ applied to the unit ball in $Y$.

*Remark* 3.3. Before defining the optimal port space on $\Gamma_{12}$, we give a short motivation for the construction procedure described below. To that end, we consider the Laplacian and define $a(v, w) := \sum_{i=1}^2 \int_{\Omega_i} \nabla v \nabla w$; we consider two components $\Omega_i \subset \mathbb{R}^2$, $i = 1, 2$, each of height $H$ in $x_2$ and length $L$ in $x_1$, such that $\Gamma_1$ is at

[3] Note that, following the common notation in the literature, we denote both the Young's modulus and the deviation by $E$ expecting that the respective meaning will be clear from the context.

$x_1 = -L$, $\Gamma_{12}$ is at $x_1 = 0$, and $\Gamma_2$ is at $x_1 = L$; we impose homogeneous Neumann conditions on $x_2 = 0$ and $x_2 = H$ in both components. Proceeding with separation of variables, we can infer that all harmonic functions for this problem are of the form

$$u(x_1, x_2) = a_0 + b_0 x_1 + \sum_{n=1}^{\infty} \cos\left(n\pi \frac{x_2}{H}\right) \left[a_n \cosh\left(n\pi \frac{x_1}{H}\right) + b_n \sinh\left(n\pi \frac{x_1}{H}\right)\right], \tag{3.4}$$

where the coefficients $a_n, b_n \in \mathbb{R}$, $n = 0, \ldots, \infty$, are determined by the Dirichlet data on $\Gamma_1$ and $\Gamma_2$. Because of the cosh function we can observe a very rapid and exponential decay of the harmonic functions (3.4) in the interior of $\Omega$. Therefore, most of the harmonic functions (3.4) have negligibly small values on $\Gamma_{12}$, which is why we expect a low-dimensional port space on $\Gamma_{12}$ to be able to provide a very good approximation of all harmonic functions (3.4). The construction procedure described below generalizes the separation of variables ansatz.

**3.1. Construction of optimal port spaces via a transfer operator.** First, we address the case where $\mathbf{g} = (0, 0, 0)^T$ and therefore $f_i(v) = 0$, $i = 1, 2$; the general case will be dealt with at the end of this subsection. Motivated by the separation of variables procedure, and the fact that the global solution $u$ on $\widetilde{\Omega}$ satisfies the PDE locally on $\Omega$, we consider the space of $a$-harmonic extensions

$$\tilde{\mathcal{H}} := \{w \in [H^1(\Omega)]^3 \,:\, a(w, v) = 0 \;\; \forall v \in X_0\}, \tag{3.5}$$

where $X_0$ has been defined in (2.3). For theoretical purposes we have to consider the quotient space $\mathcal{H} := \tilde{\mathcal{H}}/\mathcal{RB}$ instead of $\tilde{\mathcal{H}}$, where $\mathcal{RB} := \{\mathbf{a} + \mathbf{b} \times (x_1, x_2, x_3)^T, \mathbf{a}, \mathbf{b} \in \mathbb{R}^3\}$ is the space of rigid body motions (see Appendix A and the supplementary material for details on the latter). To construct an optimal port space on the shared port $\Gamma_{12}$ we therefore consider subspaces of $\mathcal{H}_{\Gamma_{12}}$, where $\mathcal{H}_\Gamma := \{u|_\Gamma, \;\; u \in \mathcal{H}\}$, $\Gamma = \Gamma_1, \Gamma_{12}, \Gamma_2$.

To assess how fast the $a$-harmonic functions decay in the interior of $\Omega$ we introduce a transfer operator $P : \mathcal{H}_{\Gamma_1 \cup \Gamma_2} \to \mathcal{H}_{\Gamma_{12}}$, which we define as follows:

$$\text{For } w \in \mathcal{H} \text{ and thus } w|_{\Gamma_1 \cup \Gamma_2} \in \mathcal{H}_{\Gamma_1 \cup \Gamma_2} \text{ we define } P(w|_{\Gamma_1 \cup \Gamma_2}) := w|_{\Gamma_{12}}. \tag{3.6}$$

For the analysis of $P$ and the remaining theoretical findings in this subsection we closely follow [3], where optimal local approximation spaces have been derived for the generalized FE method. First, we note that the operator $P$ is compact, which is proved in Appendix B (see Proposition B.2). The main ingredient of the proof is the following version of the Caccioppoli inequality, whose proof will also be provided in Appendix B.

LEMMA 3.4 (Caccioppoli inequality). *Let* $w \in [H^1(\Omega)]^3$ *satisfy*

$$a(w, v) = 0 \quad \forall v \in X_0. \tag{3.7}$$

*Then on* $\Omega^* \subsetneq \Omega^{**} \subset \Omega$ *with* $\operatorname{dist}(\partial\Omega^* \setminus \partial\Omega, \partial\Omega^{**} \setminus \partial\Omega) > \varrho > 0$ *there holds*

$$\int_{\Omega^*} \frac{\partial w^i}{\partial x_j} C_{ijkl} \frac{\partial w^k}{\partial x_l} dx \leq \frac{\|E\|_{[L^\infty(\Omega)]^3}}{E_0} \frac{12}{\varrho^2} \frac{1-\nu}{(1+\nu)(1-2\nu)} \|w\|^2_{[L^2(\Omega^{**} \setminus \Omega^*)]^3}. \tag{3.8}$$

Next, we introduce the adjoint operator $P^* : \mathcal{H}_{\Gamma_{12}} \to \mathcal{H}_{\Gamma_1 \cup \Gamma_2}$. Then the operator $P^*P$ is a compact, self-adjoint, nonnegative operator, which maps $\mathcal{H}_{\Gamma_1 \cup \Gamma_2}$ into itself. We may thus employ the Hilbert–Schmidt theorem and Theorem 2.2 in Chapter 4 of [37] to show the following result.

PROPOSITION 3.5. *Let $\varphi_j$ and $\lambda_j$ be the eigenfunctions and eigenvalues which satisfy the eigenvalue problem: Find $(\varphi_j, \lambda_j) \in (\mathcal{H}, \mathbb{R}^+)$ such that*

$$(\varphi_j|_{\Gamma_{12}}, w|_{\Gamma_{12}})_{\Gamma_{12}} = \lambda_j [(\varphi_j|_{\Gamma_1}, w|_{\Gamma_1})_{\Gamma_1} + (\varphi_j|_{\Gamma_2}, w|_{\Gamma_2})_{\Gamma_2}] \quad \forall w \in \mathcal{H}. \tag{3.9}$$

*Additionally, let the eigenvalues $\lambda_j$ be listed in nonincreasing order of magnitude, that is, $\lambda_1 \geq \lambda_2 \geq \cdots$, and $\lambda_j \to 0$ as $j \to \infty$. The optimal approximation space for $d_n(P(\mathcal{H}_{\Gamma_1 \cup \Gamma_2}); \mathcal{H}_{\Gamma_{12}})$ is given by*

$$\Lambda^n := \text{span}\{\chi_1^{sp}, \ldots, \chi_n^{sp}\}, \qquad \text{where } \chi_j^{sp} = P(\varphi_j|_{\Gamma_1 \cup \Gamma_2}), \quad j = 1, \ldots, n. \tag{3.10}$$

*Moreover, there holds*

$$d_n(P(\mathcal{H}_{\Gamma_1 \cup \Gamma_2}); \mathcal{H}_{\Gamma_{12}}) = \sup_{\xi \in \mathcal{H}_{\Gamma_1 \cup \Gamma_2}} \inf_{\zeta \in \Lambda^n} \frac{\|P\xi - \zeta\|_{\Gamma_{12}}}{\|\xi\|_{\Gamma_1 \cup \Gamma_2}} = \sqrt{\lambda_{n+1}}. \tag{3.11}$$

*Proof.* Exploiting that $P^*$ is the adjoint operator of $P$, we may reformulate (3.9) as follows: Find $(\varphi_j, \lambda_j) \in (\mathcal{H}, \mathbb{R}^+)$ such that

$$(P^* P \varphi_j|_{\Gamma_1 \cup \Gamma_2}, w|_{\Gamma_1 \cup \Gamma_2})_{\Gamma_1 \cup \Gamma_2} = \lambda_j (\varphi_j|_{\Gamma_1 \cup \Gamma_2}, w|_{\Gamma_1 \cup \Gamma_2})_{\Gamma_1 \cup \Gamma_2} \quad \forall w \in \mathcal{H}.$$

The assertion then follows from Theorem 2.2 in Chapter 4 of [37]. ∎

*Remark* 3.6. We note that this "transfer eigenproblem" is directly related to the eigenproblem introduced and analyzed in Babuška and Lipton [3] but also to more classical constructions, in particular separation of variables and the concept (say, in acoustics) of evanescence. As regards separation of variables, we return to our motivating example discussed in Remark 3.3 to establish the connection explicitly. Proceeding with separation of variables, the eigenproblem in $x_2$ yields separation constants $\sigma_j = (j\pi)/H$, $j = 0, 1, 2, \ldots$, which then inform the decay of the corresponding eigenmodes in $x_1$. We can now exploit the separation of variables solution to solve (3.9) in closed form: $\lambda_j = (\cosh(L\sigma_{j-1}))^{-2}$, $j = 1, 2, 3, \ldots$. This simple model problem also foreshadows the potentially very good performance of the associated optimal space (3.10) in light of Definition 3.1 and Proposition 3.8: we obtain exponential convergence.

Recall that so far we have considered the quotient space $\mathcal{H}$, neglecting rigid body modes. Therefore, we introduce a basis $\eta_j$, $j = 1, \ldots, 6$, of the space $\mathcal{RB}$ (see Appendix A for a possible basis, and the supplementary material for a proof that the space of rigid body motions has six dimensions) and define

$$\chi_j^{\mathcal{RB}} := \eta_j|_{\Gamma_{12}} - \sum_{j=1}^{n} (\eta_j|_{\Gamma_{12}}, \chi_j^{sp})_{\Gamma_{12}} \chi_j^{sp}. \tag{3.12}$$

As we can represent all functions in the space $\mathcal{RB}_\Omega := \{\mathbf{a} + \mathbf{b} \times (x_1, x_2, x_3)^T, \mathbf{a}, \mathbf{b} \in \mathbb{R}^3, x = (x_1, x_2, x_3)^T \in \Omega\}$, by the $a$-harmonic extensions (2.10) of $\eta_j|_{\Gamma_{12}}$, $j = 1, \ldots, 6$, and the restrictions of $\eta_j$ to $\Gamma_1$ and $\Gamma_2$ (see Lemma A.1), it is sufficient to consider the space

$$\Lambda^n_{\mathcal{RB}} := \text{span}\{\chi_1^{\mathcal{RB}}, \ldots, \chi_6^{\mathcal{RB}}, \chi_1^{sp}, \ldots, \chi_n^{sp}\} \tag{3.13}$$

to facilitate an approximation of arbitrary functions in $\tilde{\mathcal{H}} = \{w \in [H^1(\Omega)]^3 : a(w, v) = 0 \ \forall v \in X_0\}$.

Finally, we also allow $\mathbf{g} \neq (0,0,0)^T$. Note that, similarly to (2.9), we can write $u = u^f + \tilde{u}^0$, where $u^f \in X_0$ and $\tilde{u}^0 \in X$ are the solutions of

$$a(u^f, v) = f(v) \quad \forall v \in X_0, \quad \text{and} \quad a(\tilde{u}^0, v) = 0 \quad \forall v \in X_0, \quad \text{respectively.} \tag{3.14}$$

As $\tilde{u}^0 \in \tilde{\mathcal{H}}$ it can be well approximated by the space $\Lambda^n_{\mathcal{RB}}$ and it therefore remains to deal with $u^f$. Thanks to the definition of the $a$-harmonic extensions in (2.10), the definition of $b_i^f$, $i = 1, 2$, in (2.11), and the decomposition $X = X_{\Gamma_{12}} \oplus X_{1;0} \oplus X_{2;0}$, it is easy to show (see the supplementary material for a proof) that there holds $u^f = \Phi^f + b^f$, where $\Phi^f \in X_{\Gamma_{12}}$ solves

$$a(\Phi^f, \Phi_l) = f(\Phi_l) - a(b^f, \Phi_l), \quad l = 1, \dots, \infty. \tag{3.15}$$

To represent $f$ within the port space we thus set

$$\chi^f := \Phi^f|_{\Gamma_{12}} - \sum_{j=1}^{n} (\Phi^f|_{\Gamma_{12}}, \chi_j^{sp})_{\Gamma_{12}} \chi_j^{sp} - \sum_{k=1}^{6} (\Phi^f|_{\Gamma_{12}}, \chi_k^{\mathcal{RB}})_{\Gamma_{12}} \chi_k^{\mathcal{RB}}, \tag{3.16}$$

as $b^f|_{\Gamma_{12}} = 0$, and obtain that the space

$$\Lambda^{n,f}_{\mathcal{RB}} := \operatorname{span}\{\chi_1^{\mathcal{RB}}, \dots, \chi_6^{\mathcal{RB}}, \chi_1^{sp}, \dots, \chi_n^{sp}, \chi^f\} \tag{3.17}$$

is the optimal port space for the port $\Gamma_{12}$. Moreover, the space $\Lambda^{n,f}_{\mathcal{RB}}$ thus provides a good approximation of arbitrary functions in $\{w \in [H^1(\Omega)]^3 \,:\, a(w, v) = f(v) \;\forall v \in X_0\}$.

Assuming without loss of generality that $\chi^f \notin \Lambda^n_{\mathcal{RB}}$, we may now choose the orthogonal[4] reduced basis $\{\chi_k\}_{k=1}^m$ introduced in section 2.2 as

$$\chi_j = \chi_j^{\mathcal{RB}}, \;\; j = 1, \dots, 6, \quad \chi_{j+6} = \chi_j^{sp}, \;\; j = 1, \dots, n, \quad \chi_{n+7} = \chi^f. \tag{3.18}$$

We denote this basis henceforth as spectral basis, since the basis functions $\{\chi_j^{sp}\}_{j=1}^n$ are the traces of the first $n$ eigenfunctions of the transfer eigenvalue problem. Via the corresponding $a$-harmonic extensions $\{\Phi_k\}_{k=1}^{n+7}$ as introduced in (2.14), we may then define the reduced space $X^n_{\Gamma_{12}} := \operatorname{span}\{\Phi_k, k = 1, \dots, n+7\}$ and the port-reduced static condensation approximation corresponding to the optimal port space $\Lambda^{n,f}_{\mathcal{RB}}$:

$$u^n := \sum_{i=1}^{2} \big(b_i^f + \mathcal{L}_{i,\Gamma_i} u_{D,i}\big) + \sum_{k=1}^{n+7} U_k^n \Phi_k, \tag{3.19}$$

where the coefficients $U_k^n \in \mathbb{R}$ satisfy the Schur complement system (2.16) for the test space $X^n_{\Gamma_{12}}$.

[4]Note that, thanks to the Hilbert–Schmidt theorem, the functions $\{\varphi_j|_{\Gamma_1 \cup \Gamma_2}\}_{j=1}^{\infty}$ form a complete orthonormal basis for $\mathcal{H}_{\Gamma_1 \cup \Gamma_2}$, where $\varphi_j \in \mathcal{H}$ are the eigenfunctions of (3.9). As a consequence the basis functions $\{\chi_1^{sp}, \dots, \chi_n^{sp}\}$ are orthogonal with respect to the $(\cdot,\cdot)_{\Gamma_{12}}$-inner product and satisfy

$$\|\chi_j^{sp}\|^2_{\Gamma_{12}} = \lambda_j \, \|\varphi_j|_{\Gamma_1 \cup \Gamma_2}\|^2_{\Gamma_1 \cup \Gamma_2} = \lambda_j.$$

**3.2. Computational realization of the transfer eigenvalue problem.** In this subsection we outline how one can compute an approximation of the transfer eigenvalue problem and thus the optimal port space $\Lambda^{n,f}_{\mathcal{RB}}$ via the FE method.

First, we emphasize that in order to compute an approximation of the eigenvalues and eigenfunctions of (3.9), we do not need to consider the quotient space $\mathcal{H}$ but can employ the space $\tilde{\mathcal{H}}$ instead.[5]

Next, we introduce partitions of the subdomains $\Omega_i$, $i = 1, 2$, which match at the interface $\Gamma_{12}$. Moreover, we introduce a corresponding conforming FE space $X^h \subset [H^1(\Omega)]^3$ of dimension $\mathcal{N}$ with a nodal basis $\{\psi_1, \dots, \psi_{\mathcal{N}}\}$ and associated FE port spaces $\Lambda^h_{\Gamma_{12}} := \{v^h|_{\Gamma_{12}} : v^h \in X^h\}$ and $\Lambda^h_{\Gamma_1\cup\Gamma_2} := \{v^h|_{\Gamma_1\cup\Gamma_2} : v^h \in X^h\}$. Without loss of generality we assume that the first $2\mathcal{N}_\Gamma$ basis functions are associated with the nodes that lie on the Dirichlet boundary $\bar{\Sigma}_D = \bar{\Gamma}_1 \cup \bar{\Gamma}_2$, and the last $\mathcal{N}_\Gamma$ basis functions correspond to the nodes that lie on $\Gamma_{12}$. Here, $\mathcal{N}_\Gamma$ denotes the number of DOFs on the three interfaces, which we choose to be identical for the sake of simplicity. Then we may introduce the matrices $\underline{B} \in \mathbb{R}^{\mathcal{N}-2\mathcal{N}_\Gamma \times 2\mathcal{N}_\Gamma}$, $\underline{D} \in \mathbb{R}^{\mathcal{N}-2\mathcal{N}_\Gamma \times \mathcal{N}-2\mathcal{N}_\Gamma}$, and $\underline{A} \in \mathbb{R}^{\mathcal{N}\times\mathcal{N}}$, defined as

$$\underline{B}_{i,j} := a(\psi_j, \psi_i), \quad 2\mathcal{N}_\Gamma + 1 \le i \le \mathcal{N}, \;\; 1 \le j \le 2\mathcal{N}_\Gamma,$$
$$\underline{D}_{i,j} := a(\psi_j, \psi_i), \quad 2\mathcal{N}_\Gamma + 1 \le i, j \le \mathcal{N}, \qquad \underline{A} = \begin{bmatrix} \underline{I}_{2\mathcal{N}_\Gamma} & 0 \\ \underline{B} & \underline{D} \end{bmatrix},$$

where $\underline{I}_{2\mathcal{N}_\Gamma} \in \mathbb{R}^{2\mathcal{N}_\Gamma \times 2\mathcal{N}_\Gamma}$ is the identity matrix. By expressing functions $\xi^h \in \Lambda^h_{\Gamma_1\cup\Gamma_2}$ in the basis $\{\psi_1|_{\Gamma_1\cup\Gamma_2}, \dots, \psi_{2\mathcal{N}_\Gamma}|_{\Gamma_1\cup\Gamma_2}\}$ and denoting the vector containing the respective coefficients by $\underline{\xi} \in \mathbb{R}^{2\mathcal{N}_\Gamma}$, we obtain the following matrix representation $\underline{P} \in \mathbb{R}^{\mathcal{N}_\Gamma \times 2\mathcal{N}_\Gamma}$ of the transfer operator:

$$\underline{P}\,\underline{\xi} = \begin{bmatrix} 0 & \underline{I}_{\mathcal{N}_\Gamma} \end{bmatrix} \underline{A}^{-1} \begin{bmatrix} \underline{I}_{2\mathcal{N}_\Gamma} \\ 0 \end{bmatrix} \underline{\xi}, \tag{3.20}$$

where $\underline{I}_{\mathcal{N}_\Gamma} \in \mathbb{R}^{\mathcal{N}_\Gamma \times \mathcal{N}_\Gamma}$ is again the identity matrix.

Finally, we denote by $\underline{G}_{\Gamma_1\cup\Gamma_2} \in \mathbb{R}^{2\mathcal{N}_\Gamma \times 2\mathcal{N}_\Gamma}$ and $\underline{G}_{\Gamma_{12}} \in \mathbb{R}^{\mathcal{N}_\Gamma \times \mathcal{N}_\Gamma}$ the inner product matrices associated with the inner products $(\cdot,\cdot)_{\Gamma_1\cup\Gamma_2}$ and $(\cdot,\cdot)_{\Gamma_{12}}$, respectively. For details on $\underline{G}_{\Gamma_1\cup\Gamma_2}$ and $\underline{G}_{\Gamma_{12}}$ we refer the reader to the supplementary material.

Then the FE approximation of the transfer eigenvalue problem (3.9) reads as follows: Find the eigenvectors $\underline{\xi}_j \in \mathbb{R}^{2\mathcal{N}_\Gamma}$ and the eigenvalues $\lambda_j \in \mathbb{R}^+$ such that

$$\underline{P}^t \underline{G}_{\Gamma_{12}} \underline{P}\,\underline{\xi}_j = \lambda_j \, \underline{G}_{\Gamma_1\cup\Gamma_2}\, \underline{\xi}_j. \tag{3.21}$$

Note that in actual practice we would not assemble the matrix $\underline{P}$, but rather compute the harmonic extensions by successively solving the linear systems of equations

$$\underline{A}\,\underline{\tilde{u}}^0_k = \begin{bmatrix} \underline{I}_{2\mathcal{N}_\Gamma} \\ 0 \end{bmatrix} \underline{e}_k \qquad \text{for the unit vectors } \underline{e}_k \in \mathbb{R}^{2\mathcal{N}_\Gamma}, \quad k = 1, \dots, 2\mathcal{N}_\Gamma,$$

and store the evaluations of the harmonic extensions on $\Gamma_{12}$, that is, $\begin{bmatrix} 0 & \underline{I}_{\mathcal{N}_\Gamma} \end{bmatrix} \underline{\tilde{u}}^0_k$. Subsequently we would assemble and solve the generalized eigenvalue problem (3.21).

[5] Note to that end that, thanks to Lemma A.1, a basis for the space $\mathcal{RB}_\Omega$ spans an invariant subspace of $P^*P$. If the two components $\Omega_i$, $i = 1, 2$, and the three ports $\Gamma_1, \Gamma_2, \Gamma_{12}$ have the same geometry, respectively, then the first six eigenvalues of the transfer eigenvalue problem on $\tilde{\mathcal{H}}$ equal 1 and the corresponding eigenfunctions form a basis for $\mathcal{RB}_\Omega$. Thanks to the above and Lemma B.1 we obtain that the remaining eigenvalues and eigenspaces coincide with those of the generalized eigenvalue problem on $\mathcal{H}$.

The coefficients of the FE approximation of the reduced basis $\{\chi_1, \dots, \chi_{n+6}\}$ are then given by $\underline{\chi}_j = \underline{P}\,\underline{\xi}_j$, $j = 1, \dots, n+6$. To account for the right-hand side we finally solve the linear system of equations

$$\underline{D}\underline{u}^f = \underline{F}, \text{ where } \underline{F}_i = f(\psi_{i+2\mathcal{N}_\Gamma}), \quad 1 \le i \le \mathcal{N} - 2\mathcal{N}_\Gamma, \tag{3.22}$$

and define

$$\underline{\chi}_{n+7} = \begin{bmatrix} 0 & \underline{I}_{\mathcal{N}_\Gamma} \end{bmatrix} \underline{u}^f \tag{3.23}$$

if $\chi_{n+7}$ is orthogonal to $\{\chi_1, \dots, \chi_{n+6}\}$; otherwise an orthogonalization has to be performed.

*Remark* 3.7. Finally, we note that for the illustrative result based on separation of variables in Remarks 3.3 and 3.6, we observe that the respective FE approximations converge to the eigenvalues $\lambda_j$ with an order that is quadratic in the mesh size.

**3.3. A priori error bound.** The result in (3.11) can be exploited to derive an a priori error bound for the approximation error between any solution $u$ of (2.3) and the optimal sc approximation $u^n$ as stated in the following proposition.

PROPOSITION 3.8 (a priori error bound). *Let $u$ be the (exact) solution of* (2.3) *and $u^n$ the optimal sc approximation defined in* (3.19). *Then we have the following a priori error bound:*

$$\frac{\|u - u^n\|_X}{\|u\|_X} \le C_1(\Omega)\,\sqrt{\lambda_{n+1}}, \tag{3.24}$$

*where $\lambda_{n+1}$ is the $n+1$th eigenvalue of* (3.9) *and $C_1(\Omega)$ is a constant which depends neither on $u$ nor on $u^n$.*

*Proof.* The basic idea of the proof is the following: First, we use Céa's lemma to obtain

$$\|u - u^n\|_X \le \|u - u^n_{sp}\|_X, \tag{3.25}$$

where $u^n_{sp}$ lies in the same space as $u^n$ and will be constructed in such a way that we may exploit (3.11). As the parts of $u$ which represent the rigid body modes and the right-hand side $f$ can be represented exactly by $b^f$ and functions in $X^n_{\Gamma_{12}}$ (see the discussion after Remark 3.6) and thus $u^n_{sp}$, those parts cancel, and we end up with a difference between two functions in $\mathcal{H}$. Choosing the remaining coefficients appropriately allows us to apply (3.11). For a detailed proof we refer the reader to Appendix B. ∎

**4. Generalization to parametrized PDEs.** As already indicated in the introduction, many applications require a rapid simulation response for many different material parameters such as the Young's modulus in (2.7). Therefore, it is desirable to have a port-reduced sc procedure that is able to deal efficiently with parameter-dependent PDEs. Recall, however, that the optimal port space as introduced in section 3 is based on the space of functions that solve the (now parametrized) PDE and therefore also depends on the parameter. As the computation of a, say, FE approximation of $\Lambda^{n,f}_{\mathcal{RB}}$ requires solving the PDE on $\Omega$ $2\mathcal{N}_\Gamma$ times, where $\mathcal{N}_\Gamma$ denotes the number of DOFs on $\Gamma_1$ and $\Gamma_2$, constructing a new optimal port space "from scratch" for each new parameter value is in general not feasible. The goal of this section is

thus to construct a low-dimensional and quasi-optimal port space that is parameter-independent but yields an accurate approximation for the full parameter set of interest. Model order reduction and particularly RB methods [15, 17, 38] are very well suited to our goal. We generalize in section 4.4 the "standard" greedy algorithm [44] used in RB methods to a spectral greedy algorithm which constructs a reduced basis to approximate the $n$ eigenspaces associated with the $n$ largest eigenvalues of the parameter-dependent generalized (transfer) eigenvalue problem. (Quasi-)optimality of the resulting low-dimensional parameter-independent space can be inferred from the results in [9]. We finally demonstrate in section 4.5 that the spectral greedy algorithm yields a convergent port-reduced sc approximation in the sense that the relative approximation error can be bounded by any given tolerance, where the latter enters the spectral greedy algorithm as an input. To start we state the parametrized PDE of interest in section 4.1, we then recall the port-reduced sc procedure for parameter-dependent PDEs in section 4.2, and finally we generalize the findings of section 3 to the parametrized setting in section 4.3.

**4.1. Problem setting.** Let $\Omega$, $\Omega_i$, $\Gamma_i$, $i = 1, 2$, and $\Gamma_{12}$ be as in section 2. For each component $\Omega_i$, $i = 1, 2$, we define a parameter $\mu_i = (E_i, E_i^r, g^1, g^2, g^3) \in \mathcal{D}_i \subset \mathbb{R}^5$, where $\mathcal{D}_i$ denotes the parameter set of all admissible parameters associated with $\Omega_i$. We may then introduce the parametrized bilinear and linear forms $a_i(\cdot, \cdot; \mu_i) : [H^1(\Omega_i)]^3 \times [H^1(\Omega_i)]^3 \to \mathbb{R}$ and $f_i(\cdot; \mu_i) : [H^1(\Omega_i)]^3 \to \mathbb{R}$ defined as

$$a_i(w, v; \mu_i) := E_i \left\{ \int_{\Omega_{i,E_i}} \frac{\partial w^i}{\partial x_j} C_{ijkl} \frac{\partial v^k}{\partial x_l} dx + E_i^r \int_{\Omega_{i,E_i^r}} \frac{\partial w^i}{\partial x_j} C_{ijkl} \frac{\partial v^k}{\partial x_l} dx \right\},$$

$$f_i(v; \mu_i) := \int_{\Omega_i} \mathbf{g} \cdot v \, dx,$$

where $C_{ijkl}$ is defined as in section 2. Here, we choose the Young's modulus $E(x)$ as used in (2.4) and (2.7) equal to $E_i \in \mathbb{R}$ in subdomains $\Omega_{i,E_i} \subset \Omega_i$ and equal to $E_i E_i^r \in \mathbb{R}$ in the remaining parts $\Omega_{i,E_i^r} = \Omega_i \setminus \Omega_{i,E_i}$. In this way, we can consider materials that are (significantly) stiffer or softer in some parts of the (sub)domains than in the remaining parts. Note that we prescribe the same gravitational field in both components, assuming for the sake of simplicity that the mass density is constant. We shorten notation by setting $\mathcal{D} = \mathcal{D}_1 \times \mathcal{D}_2$ and $\mu = (\mu_1, \mu_2)$. Next, we introduce the global bilinear and linear forms $a(\cdot, \cdot; \mu) : [H^1(\Omega)]^3 \times [H^1(\Omega)]^3 \to \mathbb{R}$ and $f(\cdot; \mu) : [H^1(\Omega)]^3 \to \mathbb{R}$ that are defined as $a(v, w; \mu) := \sum_{i=1}^2 a_i(v, w; \mu_i)$ and $f(v; \mu) := \sum_{i=1}^2 f_i(v; \mu_i)$. We consider the following parametrized problem: For any given $\mu \in \mathcal{D}$ find $u(\mu) \in X$ such that

$$a(u(\mu), v; \mu) = f(v; \mu) \quad \forall v \in X_0. \tag{4.1}$$

Finally, we define the following (semi-)inner products and (semi)norms. First, we introduce local parameter-dependent energy semi-inner products and local induced energy seminorms as $((v, w))_{\mu,i} := a_i(v, w; \mu_i)$ and $|||v|||_{\mu,i} := ((w, w))_{\mu,i}^{1/2}$ for all $v, w \in [H^1(\Omega_i)]^3$, $i = 1, 2$. The corresponding global parameter-dependent energy inner product and energy norm are defined as $((v, w))_\mu := \sum_{i=1}^2 ((v, w))_{\mu,i}$ and $|||v|||_\mu := (\sum_{i=1}^2 |||v|||_{\mu,i}^2)^{1/2}$. Next, we introduce the reference parameters $\bar{\mu}_i = (1, 1, 0, 0, 0)$, $i = 1, 2$, assuming for the sake of simplicity that the smallest values $E_{i,min}^r, E_{i,min} \in \mathcal{D}_i$, $i = 1, 2$, equal 1. We may then define the local semi-inner products and seminorms $((v, w))_i := a_i(v, w; \bar{\mu}_i)$ and $|||v|||_i := \sqrt{((v, v))_i}$ for all $v, w \in [H^1(\Omega_i)]^3$, $i = 1, 2$,

and the corresponding global inner product and norm $((v,w)) := \sum_{i=1}^2 ((v,w))_i$ and $|||v||| := (\sum_{i=1}^2 |||v|||_i^2)^{1/2}$. Thanks to our assumptions above we have the following.

LEMMA 4.1. *Under the assumptions above and due to the definition of* $\bar{\mu}_i$, $i = 1, 2$, *there holds*

$$|||v||| \le |||v|||_\mu \le c(\mu,\bar{\mu})|||v||| \qquad \forall v \in [H^1(\Omega)]^3 \quad \text{and } c(\mu,\bar{\mu}) := \sqrt{\max_{i=1,2} E_i E_i^r}. \tag{4.2}$$

Note that for large parameter domains it might be convenient to decompose the parameter domain and define reference parameters and associated parameter-free norms for each of those (parameter) subdomains to avoid large constants $c(\mu,\bar{\mu})$.

**4.2. (Port-reduced) sc for parametrized PDEs.** To formulate the sc procedure for the parametrized setting, we first introduce Riesz representations $b_i^f(\mu_i) \in X_{i;0}$ of the right-hand side as the solutions of

$$a_i(b_i^f(\mu_i), v; \mu_i) = f_i(v;\mu_i) \quad \forall v \in X_{i;0}, i = 1, 2. \tag{4.3}$$

Next, we introduce parameter-dependent $a$-harmonic extension operators $\mathcal{L}_{i,\Gamma}(\mu_i) : [H^{1/2}(\Gamma)]^3 \to [H^1(\Omega_i)]^3$, $i = 1, 2$, such that for any $\zeta \in [H^{1/2}(\Gamma)]^3$, $\Gamma = \Gamma_1, \Gamma_{12}, \Gamma_2$, there holds

$$\begin{aligned} &a_i(\mathcal{L}_{i,\Gamma}(\mu_i)\zeta, v; \mu_i) = 0 \quad \forall v \in X_{i;0}, \\ &\text{and } \ (\mathcal{L}_{i,\Gamma}(\mu_i)\zeta)\,|_\Gamma = \zeta, \quad (\mathcal{L}_{i,\Gamma}(\mu_i)\zeta)\,|_{\Gamma^*} = 0, \ \ \Gamma \neq \Gamma^*. \end{aligned} \tag{4.4}$$

The global functions

$$\Phi_k(\mu) := \begin{cases} \mathcal{L}_{1,\Gamma_{12}}(\mu_1)\chi_k & \text{in } \Omega_1, \\ \mathcal{L}_{2,\Gamma_{12}}(\mu_2)\chi_k & \text{in } \Omega_2 \end{cases} \tag{4.5}$$

then span the space of interface functions $X_{\Gamma_{12}}(\mu) := \operatorname{span}\{\Phi_k(\mu), \ k = 1, \dots, \infty\}$ and may be employed to define a reduced space $X_{\Gamma_{12}}^m(\mu) := \operatorname{span}\{\Phi_k(\mu), \ k = 1, \dots, m\}$. We may then introduce a port-reduced static condensation approximation

$$u^m(\mu) = \sum_{i=1}^2 \big(b_i^f(\mu_i) + \mathcal{L}_{i,\Gamma_i}(\mu_i)u_{D,i}\big) + \sum_{k=1}^m U_k^m(\mu)\Phi_k(\mu), \quad m \le \infty, \tag{4.6}$$

where the coefficients $U_k^m(\mu) \in \mathbb{R}$ are the solutions of the Schur complement system

$$\sum_{k=1}^m a(U_k^m(\mu)\Phi_k(\mu), \Phi_l(\mu); \mu) = f(\Phi_l(\mu);\mu) - \sum_{i=1}^2 a_i(b_i^f(\mu_i) + \mathcal{L}_{i,\Gamma_i}(\mu_i)u_{D,i}, \Phi_l(\mu);\mu_i) \tag{4.7}$$

for $l = 1, \dots, m$.

Finally, in a slight abuse of notation we redefine the inner products $(\cdot,\cdot)_\Gamma$ and induced norms $\|\cdot\|_\Gamma$, $\Gamma = \Gamma_1, \Gamma_{12}, \Gamma_2, \Gamma_1 \cup \Gamma_2$ for the remainder of this paper as follows:

$$\begin{aligned} (\zeta,\rho)_{\Gamma_{12}} &:= \sum_{i=1}^2 a_i(\mathcal{L}_{i,\Gamma_{12}}(\bar{\mu}_i)\zeta, \mathcal{L}_{i,\Gamma_{12}}(\bar{\mu}_i)\rho; \bar{\mu}_i), \\ (\zeta,\rho)_{\Gamma_i} &:= a_i(\mathcal{L}_{i,\Gamma_i}(\bar{\mu}_i)\zeta, \mathcal{L}_{i,\Gamma_i}(\bar{\mu}_i)\rho; \bar{\mu}_i), \ \ i = 1, 2, \\ (\zeta,\rho)_{\Gamma_1\cup\Gamma_2} &:= (\zeta,\rho)_{\Gamma_1} + (\zeta,\rho)_{\Gamma_2}, \\ \|\zeta\|_\Gamma &:= \sqrt{(\zeta,\zeta)_\Gamma} \quad \text{for } \ \zeta,\rho \in [H^{1/2}(\Gamma)]^3. \end{aligned} \tag{4.8}$$

We recall that $\bar{\mu}_i$, $i = 1, 2$, are reference parameters, which were introduced at the end of section 4.1.

**4.3. Optimal port spaces for parametrized PDEs.** First, we note that for any given $\mu \in \mathcal{D}$ the respective bilinear and linear forms match the setting of sections 2 and 3. Therefore, we may define a process which applies for any given $\mu \in \mathcal{D}$ the procedure in section 3 to obtain the respective parameter-dependent quantities, employing the inner products as defined in (4.8) instead of (2.13). In detail, for a given parameter $\mu \in \mathcal{D}$, solving the parameter-dependent transfer eigenvalue problem yields for this specific parameter $\mu$ an optimal $n$-dimensional port space of spectral modes $\Lambda^n(\mu)$. Augmenting this parameter-dependent space $\Lambda^n(\mu)$ with port modes that allow us to represent the right-hand side or the rigid body modes within the reduced sc space yields the (optimal) port space $\Lambda^{n,f}_{\mathcal{RB}}(\mu)$ for this specific parameter $\mu \in \mathcal{D}$. As in (3.19) we obtain a port-reduced sc approximation $u^n(\mu)$ based on this optimal space $\Lambda^{n,f}_{\mathcal{RB}}(\mu)$. For the former, the following a priori error bound, whose proof is provided in Appendix B, holds true.

PROPOSITION 4.2 (a priori error bound). *Let $u(\mu)$ be the (exact) solution of* (4.1) *and $u^n(\mu)$ the port-reduced sc approximation corresponding to the optimal port space $\Lambda^{n,f}_{\mathcal{RB}}(\mu)$. Then we have the following a priori error bound:*

$$\frac{|||u(\mu) - u^n(\mu)|||_\mu}{|||u(\mu)|||_\mu} \leq c(\mu, \bar{\mu})\, C_1(\Omega, \mu)\, \sqrt{\lambda_{n+1}(\mu)}, \tag{4.9}$$

*where $\lambda_{n+1}(\mu)$ is the $n+1$th eigenvalue of the parameter-dependent transfer eigenvalue problem and $C_1(\Omega, \mu)$ is a constant which does not depend on $u(\mu)$.*

**4.4. A spectral greedy algorithm.** The process defined in section 4.3 yields for every $\mu \in \mathcal{D}$ the (optimal) port space $\Lambda^{n,f}_{\mathcal{RB}}(\mu)$ for this specific parameter $\mu \in \mathcal{D}$. The spectral greedy algorithm which we introduce in this subsection constructs *one* quasi-optimal parameter-independent port space $\Lambda^m$ which approximates those parameter-dependent spaces $\Lambda^{n,f}_{\mathcal{RB}}(\mu)$ with a given accuracy on a finite-dimensional training set $\Xi \subset \mathcal{D}$. In the spectral greedy algorithm we exploit the fact that, although the solutions on the component pair may vary significantly with the parameter $\mu \in \mathcal{D}$, we expect that the port spaces $\Lambda^{n,f}_{\mathcal{RB}}(\mu)$, and in particular the spectral modes that correspond to the largest eigenvalues, are much less affected by a variation in the parameter thanks to the expected very rapid decay of the higher eigenfunctions in the interior of $\Omega$.

The spectral greedy algorithm shown in Algorithm 4.1 then proceeds as we now describe. As all port spaces $\Lambda^{n,f}_{\mathcal{RB}}(\mu)$ include the rigid body port modes $\{\eta_j|_{\Gamma_{12}}\}_{j=1}^6$ by construction, we initialize $\Lambda^6$ as $\text{span}\{\eta_1|_{\Gamma_{12}}, \ldots, \eta_6|_{\Gamma_{12}}\}$.

Subsequently, we compute for all $\mu \in \Xi$ the parameter-dependent optimal port spaces $\Lambda^{n,f}_{\mathcal{RB}}(\mu)$. Motivated by the a priori bound (4.9), we choose $n$ such that there holds $c(\mu, \bar{\mu}) C_1(\Omega, \mu) \sqrt{\lambda_{n+1}(\mu)} \leq (1 - (q/p))\varepsilon$ for a given tolerance $\varepsilon$ and weighting factors $p$ and $q$, $q/p < 1$. Note that in this way we ensure that for every parameter $\mu \in \Xi$ we include all necessary information that we need to obtain a good approximation for this specific parameter. The choice of $C_1(\Omega, \mu)$, $p$, and $q$ is discussed below. After having collected all functions on $\Gamma_{12}$ that are essential to obtain a good approximation for all functions $u(\mu)|_{\Gamma_{12}}$, $\mu \in \Xi$, where $u(\mu)$ solves (4.1) for all possible Dirichlet boundary conditions, we must select a suitable basis from those functions. This is realized in an iterative manner in lines 5–14.

**Algorithm 4.1:** spectral greedy.

**input :** train sample $\Xi \subset \mathcal{D}$, tolerance $\varepsilon$, weighting factors $p, q$
**output:** set of chosen parameters $S_m$, port space $\Lambda^m$

1 **Initialize** $S_6 \leftarrow \emptyset$, $\Lambda^6 \leftarrow \operatorname{span}\{\eta_1|_{\Gamma_{12}}, \dots, \eta_6|_{\Gamma_{12}}\}$, $m \leftarrow 6$
2 **foreach** $\mu \in \Xi$ **do**
3 | Compute $\Lambda^{n,f}_{\mathcal{RB}}(\mu)$ such that $c(\mu, \bar{\mu}) C_1(\Omega, \mu) \sqrt{\lambda_{n+1}(\mu)} \leq (1 - \frac{q}{p})\varepsilon$.
4 **end**
5 **while** *true* **do**
6 | **if** $\max_{\mu \in \Xi} E(S(\Lambda^{n,f}_{\mathcal{RB}}(\mu)), \Lambda^m) \leq \varepsilon / ((p-q)\varepsilon + p C_2(\Omega, \mu) c(\mu, \bar{\mu}))$ **then**
7 | | **return**
8 | **end**
9 | $\mu^* \leftarrow \arg\max_{\mu \in \Xi} E(S(\Lambda^{n,f}_{\mathcal{RB}}(\mu)), \Lambda^m)$
10 | $S_{m+1} \leftarrow S_m \cup \mu^*$
11 | $\kappa \leftarrow \arg\sup_{\rho \in S(\Lambda^{n,f}_{\mathcal{RB}}(\mu^*))} \inf_{\zeta \in \Lambda^m} \|\rho - \zeta\|_{\Gamma_{12}}$
12 | $\Lambda^{m+1} \leftarrow \Lambda^m \cup \operatorname{span}\{\kappa\}$
13 | $m \leftarrow m + 1$
14 **end**

As in the "standard" greedy algorithm in RB methods [15, 17, 38], the spectral greedy algorithm aims at minimizing at each iteration the deviation of the set we wish to approximate from the $m$-dimensional space $\Lambda^m$ which is under construction. Note that constructing the port space such that we minimize the deviation ideally yields a deviation which is close to the Kolmogorov $n$-width and thus a (quasi-)optimal port space. Therefore, in each iteration we first identify in line 9 the port space $\Lambda^{n,f}_{\mathcal{RB}}(\mu^*)$ that maximizes $E(S(\Lambda^{n,f}_{\mathcal{RB}}(\mu)), \Lambda^m)$, $\mu \in \Xi$, where $S(\Lambda^{n,f}_{\mathcal{RB}}(\mu)) \subset \Lambda^{n,f}_{\mathcal{RB}}(\mu)$; possible choices of $S(\Lambda^{n,f}_{\mathcal{RB}}(\mu))$ will be discussed below. Subsequently, we determine in line 11 the function $\kappa \in S(\Lambda^{n,f}_{\mathcal{RB}}(\mu^*))$ that is worst approximated by the space $\Lambda^m$ and enhance $\Lambda^m$ with the span of $\kappa$. The spectral greedy algorithm terminates if for all $\mu \in \Xi$ we have $\max_{\mu \in \Xi} E(S(\Lambda^{n,f}_{\mathcal{RB}}(\mu)), \Lambda^m) \leq \varepsilon / ((p-q)\varepsilon + p C_2(\Omega, \mu) c(\mu, \bar{\mu}))$ for a constant $C_2(\Omega, \mu)$ that will be discussed shortly; this choice of stop criterion ensures that we obtain $|||u(\mu) - u^m(\mu)|||_\mu / |||u(\mu)|||_\mu \leq \varepsilon$, as will be demonstrated in the next subsection.

We remark that as Algorithm 4.1 is of the same type as the "standard" greedy algorithm in RB methods, the theoretical results which have so far been obtained for the latter (see [5, 7, 9]) apply for the spectral greedy algorithm. From these results we can infer the convergence of Algorithm 4.1. Moreover, taking the recent results in [9] as a foundation, we obtain that the space $\Lambda^m$ is (quasi-)optimal with respect to the $L^\infty$-norm over the parameter set $\Xi$. We could alternatively apply a proper orthogonal decomposition and obtain a parameter-independent port space which is optimal in the $L^2$-norm over the parameter set $\Xi$. Note, however, that in contrast to the proper orthogonal decomposition, the spectral greedy algorithm allows us to control the relative error of the sc approximation for all $\mu \in \Xi$. Regarding the choice of the training set $\Xi$, we refer the reader to the recent tutorial [15] and the references therein.

**Choice of the subset $S(\Lambda^{n,f}_{\mathcal{RB}}(\mu))$.** First, we emphasize that in contrast to the standard RB setting we have an ordering of the basis functions in $\Lambda^{n,f}_{\mathcal{RB}}(\mu)$ in terms of their approximation properties thanks to the transfer eigenvalue problem. To obtain a parameter-independent port space that yields a (very) good sc approximation already for moderate $m$ it is therefore desirable that the spectral greedy algorithm selects the more important basis functions sooner rather than later during the `while` loop. As the sorting of the basis functions in terms of their approximation properties is implicitly saved in their norms,[6] we introduce the following weighted inner product and weighted induced norm on $\Lambda^{n,f}_{\mathcal{RB}}(\mu)$:

$$(\rho(\mu),\zeta(\mu))_{\Lambda^{n,f}_{\mathcal{RB}}(\mu)} := \sum_{i=1}^{n+7} \alpha_i^\rho(\mu)\alpha_i^\zeta(\mu) \quad \text{and} \quad \|\rho(\mu)\|_{\Lambda^{n,f}_{\mathcal{RB}}(\mu)} := \sqrt{(\rho(\mu),\rho(\mu))_{\Lambda^{n,f}_{\mathcal{RB}}(\mu)}}$$
$$\text{for } \rho(\mu) = \sum_{i=1}^{n+7} \alpha_i^\rho(\mu)\chi_i(\mu),\ \ \zeta(\mu) = \sum_{i=1}^{n+7} \alpha_i^\zeta(\mu)\chi_i(\mu) \in \Lambda^{n,f}_{\mathcal{RB}}(\mu), \tag{4.10}$$

where we recall that $\{\chi_i(\mu)\}_{i=1}^{n+7}$ denotes the spectral basis of $\Lambda^{n,f}_{\mathcal{RB}}(\mu)$. We thus propose considering

$$S(\Lambda^{n,f}_{\mathcal{RB}}(\mu)) := \{\zeta \in \Lambda^{n,f}_{\mathcal{RB}}(\mu) \,:\, \|\zeta\|_{\Lambda^{n,f}_{\mathcal{RB}}(\mu)} \le 1\} \tag{4.11}$$

in the spectral greedy algorithm. The deviation $E(S(\Lambda^{n,f}_{\mathcal{RB}}(\mu)),\Lambda^m)$ can then be computed by solving the following eigenvalue problem:[7] Find $(\phi_j(\mu),\sigma_j(\mu)) \in \Lambda^{n,f}_{\mathcal{RB}}(\mu) \times \mathbb{R}^+$ such that

$$\left(\phi_j(\mu) - \sum_{k=1}^m (\phi_j(\mu),\chi_k)_{\Gamma_{12}}\chi_k, \rho - \sum_{k=1}^m (\rho,\chi_k)_{\Gamma_{12}}\chi_k\right)_{\Gamma_{12}} = \sigma_j(\mu)(\xi_j(\mu),\rho)_{\Lambda^{n,f}_{\mathcal{RB}}(\mu)} \quad \forall \rho \in \Lambda^{n,f}_{\mathcal{RB}}(\mu), \tag{4.12}$$

where $\{\chi_k\}_{k=1}^m$ denotes the orthonormal basis of $\Lambda^m$. Observe that we have two different inner products on the left- and right-hand sides of (4.12). We thus obtain $E(S(\Lambda^{n,f}_{\mathcal{RB}}(\mu)),\Lambda^m) = \sqrt{\sigma_1(\mu)}$ for all $\mu \in \Xi$, and $\kappa = \phi_1(\mu^*)$ at each iteration. Note that by exploiting the definition of $(\cdot,\cdot)_{\Lambda^{n,f}_{\mathcal{RB}}(\mu)}$ in (4.10), by expressing $\phi_j$ in (4.12) in the spectral basis $\{\chi_i(\mu)\}_{i=1}^{n+7}$ of $\Lambda^{n,f}_{\mathcal{RB}}(\mu)$, and by denoting the vector containing the corresponding coefficients by $\underline{\phi}_j \in \mathbb{R}^{n+7}$, we can express the matrix version of (4.12) as follows: Find $(\underline{\phi}_j(\mu),\sigma_j(\mu)) \in (\mathbb{R}^{n+7},\mathbb{R}^+)$ such that

$$\underline{Z}(\mu)\underline{\phi}_j(\mu) = \sigma_j(\mu)\underline{\phi}_j(\mu), \tag{4.13}$$

where

$$\underline{Z}_{i,l}(\mu) := \left(\chi_l(\mu) - \sum_{k=1}^m (\chi_l(\mu),\chi_k)_{\Gamma_{12}}\chi_k, \chi_i(\mu) - \sum_{k=1}^m (\chi_i(\mu),\chi_k)_{\Gamma_{12}}\chi_k\right)_{\Gamma_{12}}. \tag{4.14}$$

[6] Recall that the basis functions $\{\chi_1^{sp}(\mu),\dots,\chi_n^{sp}(\mu)\}$ are orthogonal with respect to the $(\cdot,\cdot)_{\Gamma_{12}}$-inner product and satisfy $\|\chi_j^{sp}(\mu)\|^2_{\Gamma_{12}} = \lambda_j(\mu)\,\|\varphi_j(\mu)|_{\Gamma_1\cup\Gamma_2}\|^2_{\Gamma_1\cup\Gamma_2} = \lambda_j(\mu)$.

[7] Note to that end that there holds

$$\sup_{\rho\in S(\Lambda^{n,f}_{\mathcal{RB}}(\mu))} \inf_{\zeta\in\Lambda^m} \|\rho-\zeta\|_{\Gamma_{12}} = \sup_{\rho\in\Lambda^{n,f}_{\mathcal{RB}}(\mu),\|\rho\|_{\Lambda^{n,f}_{\mathcal{RB}}(\mu)}=1} \inf_{\zeta\in\Lambda^m} \|\rho-\zeta\|_{\Gamma_{12}} = \sup_{\rho\in\Lambda^{n,f}_{\mathcal{RB}}(\mu)} \inf_{\zeta\in\Lambda^m} \frac{\|\rho-\zeta\|_{\Gamma_{12}}}{\|\rho\|_{\Lambda^{n,f}_{\mathcal{RB}}(\mu)}}.$$

To further motivate this choice of $S(\Lambda^{n,f}_{\mathcal{RB}}(\mu))$ let us assume that all spectral modes in $\Lambda^{n,f}_{\mathcal{RB}}(\mu)$ are orthogonal to the space $\Lambda^m$ for all $\mu \in \Xi$, which is the case, for instance, for $m = 6$ but also often for higher $m$. In this case the matrices $\underline{Z}(\mu)$ reduce to diagonal matrices with diagonal entries $\underline{Z}_{i,i}(\mu) = \|\chi_i(\mu)\|^2_{\Gamma_{12}}$, $i = 1, \ldots, n+7$, $\mu \in \Xi$. A spectral greedy algorithm based on $E(S(\Lambda^{n,f}_{\mathcal{RB}}(\mu)), \Lambda^m)$ would therefore select the parameter $\mu^*$ such that the associated function $\phi_1(\mu^*)$ has maximal energy with respect to the $(\cdot,\cdot)_{\Gamma_{12}}$-inner product. Note that this is consistent with our aim to include the weighting induced by the transfer eigenvalue problem into the basis selection process by the spectral greedy algorithm.

*Remark* 4.3. Note that were we to consider the norm $\|\cdot\|_{\Gamma_{12}}$ in (4.11) and therefore the $(\cdot,\cdot)_{\Gamma_{12}}$-inner product on the right-hand side in (4.12), the sorting of the spectral basis $\{\chi_i(\mu)\}_{i=1}^{n+7}$ of $\Lambda^{n,f}_{\mathcal{RB}}(\mu)$ in terms of approximation properties is neglected in the `while` loop of Algorithm 4.1. As a consequence it may and often would happen in actual practice, also due to numerical inaccuracies, that a spectral greedy algorithm based on the $\|\cdot\|_{\Gamma_{12}}$-norm in (4.11) selects first functions that have been marked by the transfer eigenvalue problem as *less* important. Therefore, we would observe an approximation behavior of the sc approximation based on the so-constructed port space that is not satisfactory for moderate $m$. Hence, we suggest considering $S((\Lambda^{n,f}_{\mathcal{RB}}(\mu)))$ as defined in (4.11), which yields a port space with excellent approximation properties, as will be demonstrated in section 6.

**Discussion of the constants $C_1(\Omega,\mu)$ and $C_2(\Omega,\mu)$ and the weighting factors $p$ and $q$.** Sharp estimates for the constants $C_1(\Omega,\mu)$ and $C_2(\Omega,\mu)$ can be obtained by considering suitable eigenvalue problems on the component pair. This procedure, however, requires some technicalities which are beyond the scope of this paper and will therefore be addressed in another article [42]. As we expect the constants $C_1(\Omega,\mu)$ and $C_2(\Omega,\mu)$ to have the same order for most systems, it might be convenient to choose, say, $C_1(\Omega,\mu) = C_2(\Omega,\mu) = 1$. Note that another value of those constants would just result in an appropriately scaled tolerance $\varepsilon$.

We now discuss the choice of $p$ and $q$. We shall show in Theorem 4.4 (in the next subsection, and Appendix B.2) that a sufficient condition for convergence of the sc approximation associated with $\Lambda^m$ for all $\mu \in \Xi$ is

$$p > q \geq \max_{\mu\in\Xi} \theta(\mu), \tag{4.15}$$

where

$$\theta(\mu) := \left( \min_{i=1,\ldots,n+7} \|\chi_i(\mu)\|_{\Gamma_{12}} \right)^{-1} \quad \text{and there holds } \|\rho\|_{\Lambda^{n,f}_{\mathcal{RB}}(\mu)} \leq \theta(\mu)\|\rho\|_{\Gamma_{12}}. \tag{4.16}$$

We note, however, that $\theta(\mu)$ generally equals $\lambda_n^{-1/2}(\mu)$, and thus if we choose $p$ and $q$ to satisfy (4.15), the right-hand side in line 6 is about $\varepsilon\lambda_n^{-1/2}(\mu)$ and thus on the order of $\varepsilon^2$ per Proposition 4.2 and line 3 of Algorithm 4.1. Although, based on our numerical experiments, it seems that this choice is numerically manageable for given tolerances $\varepsilon$ that are equal to or larger than about $10^{-7}$, the space $\Lambda^m$ becomes in general unnecessarily large due to the very pessimistic factor $\theta(\mu)$. In actual practice it seems sufficient to choose $q = 1$ and, say, $p = 2$ to obtain a relative approximation error $|||u(\mu) - u^m(\mu)|||_\mu / |||u(\mu)|||_\mu$ which lies below the given tolerance $\varepsilon$. We also check on a test parameter sample $\mu \in \Xi_{test}$ that the desired accuracy

is indeed achieved; the latter thus serves as an empirical a posteriori substitute for the pessimistic a priori theoretical result of Theorem 4.4. Note that, assuming an exponential decay of the deviation during the spectral greedy algorithm, the choice $q = 1$ and $p = 2$ roughly corresponds to using half the number of basis functions as required by (4.15) for a provable convergence. In spite of this relaxed termination criterion, numerical experiments confirm that the choice $q = 1$ and $p = 2$ indeed yields excellent approximation results.

**4.5. Convergence of the port-reduced static condensation procedure based on a port space generated by the spectral greedy.** We consider the parameter-independent port space $\Lambda^m$ constructed by the spectral greedy Algorithm 4.1. Exploiting the design of the spectral greedy algorithm, we are able to prove the convergence of the port-reduced sc approximation as stated in the following theorem. Note that the theorem supposes the choice $p > q \geq \max_{\mu\in\Xi}\theta(\mu)$, which is not the best choice in practice, as described in the previous paragraph.

THEOREM 4.4 (convergence of the port-reduced sc procedure). *Let $u(\mu)$ be the exact solution of* (2.3) *and $u^m(\mu)$ the sc approximation as defined in* (4.6)*. Moreover, let $\varepsilon$ be a given tolerance which enters the spectral greedy Algorithm* 4.1 *as an input parameter, and $\Xi \subset \mathcal{D}$ the finite train sample employed in Algorithm* 4.1*. If we choose $p > q \geq \max_{\mu\in\Xi}\theta(\mu)$, then there holds for each $\mu \in \Xi$ and any given tolerance $\varepsilon > 0$*

$$|||u(\mu) - u^m(\mu)|||_\mu \leq \varepsilon |||u(\mu)|||_\mu. \tag{4.17}$$

*Proof.* We provide only the basic idea at this point; for the complete proof, see Appendix B. First, we use Céa's lemma to infer $|||u(\mu)-u^m(\mu)|||_\mu \leq |||u(\mu)-\hat{u}^m(\mu)|||_\mu$, where $\hat{u}^m(\mu)$ lies in the same space as $u^m(\mu)$. Then we introduce a spectral approximation as in the proof of Proposition 3.8 corresponding to the optimal port space $\Lambda^{n,f}_{\mathcal{RB}}(\mu)$ and apply the triangle inequality. Choosing the coefficients of the spectral approximation appropriately allows us to use (3.11). Subsequently, we choose the coefficients of $\hat{u}^m(\mu)$ such that we can exploit that the spectral greedy Algorithm 4.1 ensures that $\max_{\mu\in\Xi} E(S(\Lambda^{n,f}_{\mathcal{RB}}(\mu)), \Lambda^m) \leq \varepsilon/((p-q)\varepsilon + pC_2(\Omega,\mu)c(\mu,\bar{\mu}))$. ∎

**5. Generalization to arbitrary systems.** In this section, we outline the changes that have to be implemented from both an algorithmic and an analytic point of view if we now take into account that $\Omega$—and thus our component pair—is actually part of a large system of many components associated with $\widehat{\Omega}$. To allow a maximal topological flexibility in the online stage where the system is assembled, we do not in general know the size, the composition, or the shape of the system in the offline stage during which we prepare the reduced model. Therefore, to construct the port spaces, we consider in the offline stage component pairs associated with every possible configuration at a port that may be encountered in the online system. We are thus in the situation of the preceding sections: We consider a pair of two subdomains, $\Omega_1$ and $\Omega_2$, that share one port and form the domain $\Omega$, which is in turn a subdomain of a larger domain $\widehat{\Omega}$.[8]

To avoid technical details we first present the generalized results for systems of $I$ components that have the same geometry, have the same port type, and have two ports, and where all component pairs that share a port have the same geometry. We describe briefly at the end of this section how the procedures and theoretical results

[8]Note, however, that if it is known already in the offline stage that, say, a component (type) will not intersect with the boundary of the computational domain of the online system, we may also consider systems of more than two components for the generation of the port modes.

can be adjusted to the general case. We abuse notation and denote the exact solution again by $u(\mu)$ and the port-reduced sc approximation by $u^m(\mu)$. The energy norm $|||\cdot|||_\mu$ is then defined as $|||v|||_\mu := (\sum_{i=1}^I |||v|||_{\mu,i}^2)^{1/2}$ for $v \in [H^1(\widehat{\Omega})]^3$. Finally, we introduce a set $\Pi$ which contains all ports within the online system and denote an element of $\Pi$ by $\Gamma$. Super- or subscripts $\Gamma$ indicate the correspondence of a quantity or function to that specific port.

Thanks to these assumptions it is sufficient to perform the spectral greedy algorithm for one component pair. Following the procedure described in sections 3 and 4, we construct for all $\mu \in \Xi$ an optimal port space $\Lambda_{\mathcal{RB}}^{n,f}(\mu)$. Motivated by the following a priori bound, whose proof is provided in Appendix B, the sizes of the port spaces $\Lambda_{\mathcal{RB}}^{n,f}(\mu)$ in the spectral greedy algorithm are chosen such that $\Gamma_p c(\mu,\bar{\mu})\tilde{C}_1(\Omega,\mu)\sqrt{\lambda_{n+1}(\mu)} \le (1-\frac{q}{p})\varepsilon$. Here, $\Gamma_p$ is an upper bound for the number of ports in the online system.

COROLLARY 5.1 (a priori bound for systems). *Let $u(\mu)$ be the (exact) solution and $u^{n_\Gamma}(\mu)$ an sc-type approximation which uses the optimal port space $\Lambda_{\mathcal{RB},\Gamma}^{n_\Gamma,f}(\mu)$ for each port $\Gamma \in \Pi$. Then we have the following a priori error bound:*

$$\frac{|||u(\mu)-u^{n_\Gamma}(\mu)|||_\mu}{|||u(\mu)|||_\mu} \le \Gamma_p \max_{\Gamma\in\Pi}\left(c_\Gamma(\mu,\bar{\mu})\,\tilde{C}_{\Gamma,1}(\Omega_\Gamma,\mu)\,\sqrt{\lambda_{\Gamma,n+1}(\mu)}\right). \tag{5.1}$$

*Here, the constant $\tilde{C}_{\Gamma,1}(\Omega_\Gamma,\mu)$ depends only on the configuration of the component pair and not on the global system or on $u(\mu)$.*

The spectral greedy algorithm then proceeds as described in section 4.4 and terminates if we have for all $\mu \in \Xi$ that $E(S(\Lambda_{\mathcal{RB}}^{n,f}(\mu)),\Lambda^m) \le \varepsilon/((p-q)\varepsilon + p\Gamma_p\tilde{C}_2(\Omega,\mu)c(\mu,\bar{\mu}))$. It returns a parameter-independent port space $\Lambda^m$ which is used for the sc procedure on all ports in the online system. Based on that we can also show the convergence of the port-reduced sc approximation for systems as stated in the following corollary, whose proof is given in Appendix B.

COROLLARY 5.2 (convergence of the port-reduced sc procedure for systems). *Let $u(\mu)$ be the exact solution and $u^m(\mu)$ the sc approximation. Moreover, let $\varepsilon$ be a given tolerance which enters the spectral greedy algorithm as an input parameter, and $\Xi \subset \mathcal{D}$ the finite train sample employed in the spectral greedy algorithm. If we choose $p > q \ge \max_{\mu\in\Xi}\theta(\mu)$, then there holds for each $\mu \in \Xi$ and any given tolerance $\varepsilon > 0$*

$$|||u(\mu)-u^m(\mu)|||_\mu \le \varepsilon |||u(\mu)|||_\mu. \tag{5.2}$$

Note that, thanks to the expected rapid decay of the higher eigenfunctions in the parametrized transfer eigenvalue problem in the interior of $\Omega$, we anticipate in actual practice a much better scaling of the approximation error in $|\Pi|$, which is demonstrated in the numerical examples in section 6.

Finally, we briefly address arbitrary systems. In the event that we want to allow, say, $\mathcal{P}$ different port types in the online system, we apply at the offline stage the spectral greedy Algorithm 4.1 separately for each different port type and construct $\mathcal{P}$ different optimal spaces. The port spaces in each spectral greedy algorithm are constructed such that $\mathcal{P}\Gamma_p^j c(\mu,\bar{\mu})\tilde{C}_1^j(\Omega,\mu)\sqrt{\lambda_{n+1}(\mu)} \le (1-\frac{q}{p})\varepsilon$ is satisfied for all $j = 1,\dots,\mathcal{P}$. Here, $\Gamma_p^j$ denotes an upper bound for the number of ports of port type $j$ that are expected in the online system. Moreover, one requires the spectral greedy algorithm to stop if $\max_{\mu\in\Xi} E(S(\Lambda_{\mathcal{RB}}^{n,f}(\mu)),\Lambda^m) \le \varepsilon/((p-q)\varepsilon + p\sum_{j=1}^{\mathcal{P}}\Gamma_p^j\tilde{C_2}^j(\Omega,\mu)c(\mu,\bar{\mu}))$ holds.

Note that due to the definition of the inner product $(\cdot,\cdot)_\Gamma$, two ports that have the same geometry but whose associated component pairs have a different geometry or PDEs with different coefficient functions are considered as being of different port type. However, this can be relaxed by considering a different inner product on the ports which is continuous with respect to the $\|\cdot\|_\Gamma$-norm.

If one wants to consider components that have more than two ports, one just has to increase the number of ports on which arbitrary Dirichlet boundary conditions are considered in the PDE and the transfer eigenvalue problem. The thresholds in the spectral greedy algorithm in lines 3 and 6 do not need to be changed unless having more than two ports within the components increases the number of port types.

Finally, we emphasize that systems of arbitrary shape can be treated as long as the ports do not intersect. As indicated above the generalization to this case is the subject of a forthcoming paper. Note that although the determination of the exact thresholds in the spectral greedy algorithm can be challenging, the fact that numerical experiments show only a (very) weak dependence on $|\Pi|$ might indicate that in actual practice it might not be necessary to employ the exact thresholds, but rather a (rough) estimate to obtain a port space with excellent approximation properties.

**6. Numerical experiments.** In this section we demonstrate the excellent approximation properties of the (quasi-)optimal port spaces $\Lambda^{n,f}_{\mathcal{RB}}(\mu)$ and $\Lambda^m$. The focus of section 6.2 is the analysis of the eigenvalues and eigenfunctions of the transfer eigenvalue problem; we show the very rapid and exponential convergence of the eigenvalues for an I-beam with a crack. In section 6.3 we provide a thorough investigation of the spectral greedy Algorithm 4.1 and demonstrate for a stiffened plate the very fast and exponential convergence of the port-reduced sc procedure based on $\Lambda^m$. We begin in section 6.1 with a short outline of a possible computational realization of the spectral greedy algorithm. Our implementation is based on the finite element library `libMesh` [27] and uses `rbOOmit` [28]. For the solution of the (generalized) eigenvalue problems we have employed the (generalized) self-adjoint eigensolver of the `Eigen` library [13]. Note finally that we employ also for approximated quantities the same notation used until now to improve readability.

**6.1. Computational realization of the spectral greedy algorithm.** To compute an approximation of the parametrized transfer eigenvalue problems, we employ the scRBE method [12, 22, 41]. In detail, we use a Petrov–Galerkin formulation[9] both to compute $2\mathcal{N}_\Gamma$ approximations of the solutions $u(\mu) \in [H^1(\Omega)]^3$ of $a(u(\mu), v; \mu) = 0$ and of the functions $\Phi^f(\mu)$. Recall that $\mathcal{N}_\Gamma$ denotes the number of DOFs on $\Gamma_1, \Gamma_2, \Gamma_{12}$, respectively, and note that we compute for every basis function on $\Gamma_1 \cup \Gamma_2$ an associated $a$-harmonic solution as indicated in section 3.2. The tolerance for the greedy algorithm to construct the RB approximations within the scRBE method has been set to $10^{-7}$, and we use all constructed RB basis functions such that the RB approximation does not affect the convergence behavior.

Moreover, we have used the constants $\Gamma_p = C_1(\Omega, \mu) = C_2(\Omega, \mu) = 1$ in the numerical experiments. Furthermore, we have employed $q = 1$ and $p = 2$ in the numerical experiments, adjusting the tolerance $\varepsilon$ by assessing the relative approximation error for certain parameters in a test training sample. Note that the eigenvalue problems (4.12) are only of size $n+7 \times n+7$ and can therefore efficiently be solved by, say, a direct solver for each $\mu \in \Xi$. We note finally that in general the computation of the optimal port spaces $\Lambda^{n,f}_{\mathcal{RB}}(\mu)$ for all $\mu \in \Xi$ in line 3 requires far more computational time than the subsequent `while` loop.

[9] For the exact formulation and a comparison with a Galerkin formulation, see [41].

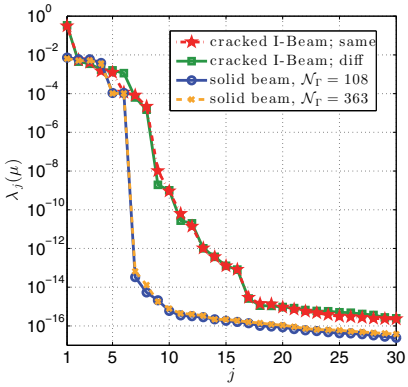


FIG. 6.1. *Eigenvalues $\lambda_j(\mu)$ for the solid beam and the I-beam with two cracks on the same and different flanges for $E_i = E_i^r = 1$, $i = 1, 2$.*

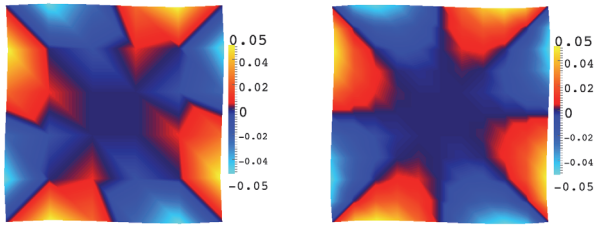

(a) $\mathcal{N}_\Gamma = 108$ (b) $\mathcal{N}_\Gamma = 363$

FIG. 6.2. *Plots of $(\chi_4^{sp}(\mu))^3$ for the solid beam, $E_1 = E_2 = E_1^r = E_2^r = 1$ and FE port space dimensions* (a) $\mathcal{N}_\Gamma = 108$ *and* (b) $\mathcal{N}_\Gamma = 363$. *Note that $(\chi_4^{sp}(\mu))^1$ and $(\chi_4^{sp}(\mu))^2$ are negligible and the superscript $j$ indicates here the $j$th component of the vector.*

**6.2. Analysis of the transfer eigenvalue problem for systems of beams.** First, we analyze the eigenvalues and eigenfunctions of the (parametrized) transfer eigenvalue problem for a solid beam and subsequently an I-beam with an internal crack.

In detail we consider a two-component system of two identical solid beam components and thus components with a separable geometry: $\Omega_1 = (-0.5, 0.5) \times (-0.5, 0.5) \times (0, 5)$ and $\Gamma_1 = (-0.5, 0.5) \times (-0.5, 0.5) \times \{0\}$. We compare two different FE discretizations of $\mathcal{N} = 3348$ and $\mathcal{N} = 22143$ DOFs per component and $\mathcal{N}_\Gamma = 108$ and $\mathcal{N}_\Gamma = 363$, respectively. Recall that $\mathcal{N}$ was introduced in section 3.2. Moreover, we consider $E_i = E_i^r = 1$, $i = 1, 2$. First, we observe a very rapid convergence of the eigenvalues yielding $\lambda_7(\mu) < 10^{-13}$ for both discretizations (see Figure 6.1), demonstrating the possible good approximation properties of $\Lambda_{\mathcal{RB}}^{n,f}(\mu)$. Recall that the eigenvalues depicted in Figure 6.1 do not correspond to the rigid body modes, which must be included in addition (see the discussion after Remark 3.6). Additionally, we see that the difference between the eigenvalues for the two FE discretizations is relatively small; the largest relative difference is encountered for the third eigenvalue and amounts to 0.1608. Comparing the spectral modes $\chi_4^{sp}(\mu)$ for the two discretizations shows that in spite of the relatively coarse mesh in Figure 6.2(a), which affects the shape of the function, the essential behavior of the spectral mode is already captured for $\mathcal{N}_\Gamma = 108$. We shall thus restrict our attention to this computationally more convenient coarser mesh.

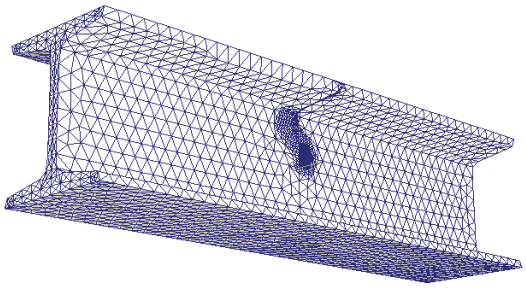

FIG. 6.3. *Component mesh for the I-beam with a crack.*

Next, we consider an I-Beam component with an internal crack as depicted in Figure 6.3 to demonstrate how the proposed method accommodates nonseparable and irregular geometries. The underlying FE discretization has $\mathcal{N} = 20490$ DOFs (for one component) and a port space dimension of $\mathcal{N}_\Gamma = 507$. We connect two identical cracked I-beam components to generate a port space and consider $E_i = E_i^r = 1$, $i = 1, 2$. The extremely rapid convergence of the eigenvalues $\lambda_j(\mu)$, $j = 1, \ldots, n$, both for an I-beam with two cracks on the *same* flange and an I-beam where the two cracks are on *different* flanges can be observed in Figure 6.1. For instance, for the former we obtain $\lambda_9(\mu) \approx 1.0152 \cdot 10^{-8}$. In light of Proposition 3.8, this demonstrates the excellent approximation properties of the port spaces $\Lambda^{n,f}_{\mathcal{RB}}(\mu)$.

Finally, we compare the spectral modes generated by the spectral greedy Algorithm 4.1 with other port modes, demonstrating the superior convergence of the former. In detail, we compare the relative error of the port-reduced sc approximation for port spaces comprising "Legendre polynomial"-type functions[10] [11], empirical port modes constructed by a pairwise training algorithm[11] [11, 12], and the spectral modes introduced in this paper. We consider the FE discretization with $\mathcal{N} = 3348$ DOFs and $\mathcal{D}_i = [1, 10] \times [1, 1] \times [-1, 1] \times [-1, 1] \times [-1, 1]$ and thus a Young's modulus which is uniform in each subdomain but possibly different in the two components. Recall that we prescribe the same gravitational vector $\mathbf{g}$ in both components. Within the spectral greedy algorithm we have considered 200 parameter values sampled from the uniform distribution over $\mathcal{D}$ and $\varepsilon = 1 \cdot 10^{-6}$. On average the port spaces $\Lambda^{n,f}_{\mathcal{RB}}(\mu)$ have had a size of 13.65, while the largest and smallest sizes encountered have been 14 and 13, respectively. Finally, the resulting parameter-independent port space $\Lambda^m$ has a size of 56. As the basis functions of the parameter-dependent port spaces $\Lambda^n(\mu)$ vary only slightly for different $\mu \in \mathcal{D}$, it seems that a significant part of the basis functions of $\Lambda^m$ have been added during the spectral greedy algorithm to represent the right-hand side $f(\cdot; \mu)$ associated with $\mathbf{g}$.

In the online stage we consider $E_i = E_i^r = 1$, $i = 1, 2$, $\mathbf{g} = (0, 0, 0)^T$, and prescribe $u_{D,1} = (0, 0, 0)^T$ and $u_{D,2} = (1, 1, 1)^T$, recalling that $u_{D,i} \in [H^{1/2}(\Gamma_i)]^3$ accounts for (non)homogeneous Dirichlet boundary conditions. We observe in Figure 6.4 that the Legendre modes perform by far the worst, demonstrating that including information on the solution manifold on the ports in the basis construction procedure can significantly improve the approximation behavior. We remark that the Legendre modes

[10] Note that each component of the displacement is the solution of a scalar singular Sturm–Liouville eigenproblem.

[11] Following the notation in [12] we have chosen $N_{\text{samples}} = 500$ and $\gamma = 3$ in the pairwise training algorithm.

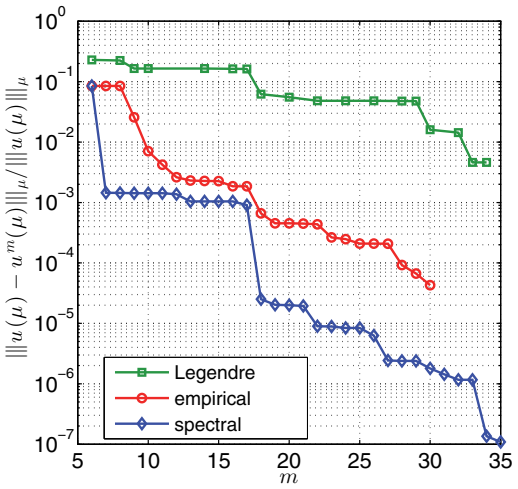


FIG. 6.4. $|||u(\mu) - u^m(\mu)|||_\mu / |||u(\mu)|||_\mu$ *for the Legendre, empirical, and spectral port modes for the solid beam.*

will perform even worse in the case of less regular behavior on the port, which further justifies the need for problem-specific port spaces in the sense of model reduction. The empirical modes and spectral modes exhibit a comparable convergence until $m = 17$, but for $m > 17$ the relative error in the spectral approximation is one order of magnitude smaller than that of the empirical port mode approximation. This can be explained by the fact that, thanks to its conception, the pairwise training algorithm is able to identify and include the most significant modes, but (in contrast to the spectral greedy algorithm) might have difficulties detecting subtle modes that affect the shape of the function at the port $\Gamma_{12}$ only slightly. Note that the temporary stagnation of the relative error for $m = 7, \ldots, 17$ for the spectral modes is due to the fact that the spectral greedy prepares the port space for all possible boundary conditions and parameter configurations. Thus for the boundary conditions considered here some spectral modes, as, say, a mode related to a twisting (torsion) of the beam, are not needed for the approximation.

**6.3. Demonstration of the spectral greedy algorithm for a simplified model for ship stiffeners.** For motivation purposes, we first consider a plate consisting of two components with $\Omega_1 = (-0.7, 0.7) \times (-0.05, 0.05) \times (-0.6, 0.6)$, $\Omega_2 = (0.7, 1.4) \times (-0.05, 0.05) \times (-0.6, 0.6)$, $\Gamma_1 = \{-0.7\} \times (-0.05, 0.05) \times (-0.6, 0.6)$, $\Gamma_2 = \{1.4\} \times (-0.05, 0.05) \times (-0.6, 0.6)$, and uniform Young's modulus $E_i = E_i^r = 1$, $i = 1, 2$, $\mathbf{g} = (0, 0, 0)^T$. We apply zero Dirichlet boundary conditions on $\Gamma_1$ and $\eta_4|_{\Gamma_2} / \|\eta_4|_{\Gamma_2}\|_{\Gamma_2} = (x_2, 0, 0)^T / \|\eta_4|_{\Gamma_2}\|_{\Gamma_2}$ on $\Gamma_2$. We observe that the plate sags in the interior of the domain (see Figure 6.5(a)), where $\Gamma_2$ can be seen in the foreground of the picture. To increase the stiffness and stability of plates or shells, it is a common engineering practice to attach stiffeners such as beams (see, for instance, [43] and references therein). In this subsection we consider a simplified ship stiffener component as depicted in Figure 6.5(c) with $\Omega_2 = (0.7, 1.4) \times (-0.05, 0.05) \times (-0.6, 0.6)$ and $\Gamma_2 = \{1.4\} \times (-0.05, 0.05) \times (-0.6, 0.6)$, the latter indicated in yellow, allowing Young's modulus ratio $E_i^r$ to vary between 1 and 20 in the dark (red) shaded areas. Note that for $E_i^r = 1$ we obtain the setting as considered in the beginning of this subsection. The underlying FE discretization of $\Omega_2$ is also the same as above and

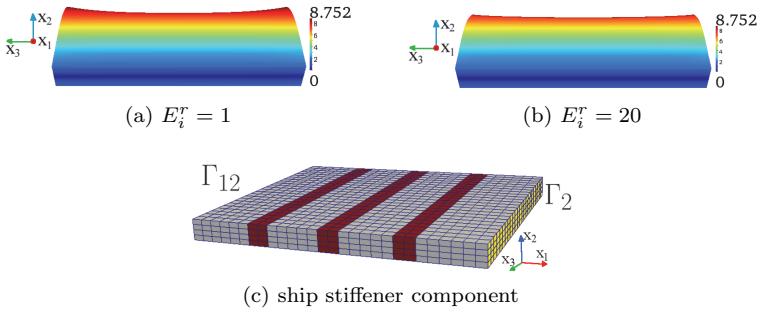


(a) $E_i^r = 1$ (b) $E_i^r = 20$

(c) ship stiffener component

FIG. 6.5. *Plots of the magnitude of the displacement for a* (a) *nonstiffened and* (b) *stiffened plate for the motivating example at the beginning of section* 6.3. (c) *Component mesh of the ship stiffener; the port* $\Gamma_2$ *is indicated in yellow. In the dark (red) shaded bands, Young's modulus (ratio) may be varied between* 1 *and* 20. *(Color available online.)*

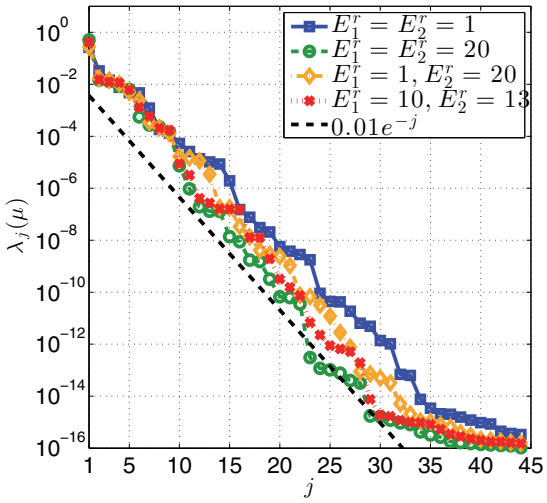


FIG. 6.6. *Eigenvalues* $\lambda_j(\mu)$ *for different Young's modulus ratios* $E_i^r$, $i = 1, 2$.

has $\mathcal{N} = 13125$ DOFs and a port space with dimension $\mathcal{N}_\Gamma = 375$. We then connect two ship stiffener components, prescribe the same Dirichlet boundary conditions as above, and again prescribe $\mathbf{g} = (0, 0, 0)^T$, $E_i = 1$, but $E_i^r = 20$, $i = 1, 2$. Now we see in Figure 6.5(b) that the deflection of the plate (observed for the uniform Young's modulus) has disappeared to a great extent. We would therefore expect a faster convergence of the eigenvalues $\lambda_j(\mu)$ of the parametrized transfer eigenvalue problem for the stiffened plate, which can indeed be seen in Figure 6.6. In general, we observe for the ship stiffener application an exponential convergence of order $\approx e^{-j}$ of the eigenvalues $\lambda_j(\mu)$, demonstrating again the outstanding approximation properties of $\Lambda_{\mathcal{RB}}^{n,f}(\mu)$.

Next, we analyze the parameter selection of the spectral greedy Algorithm 4.1 and provide in this context also a comparison of the eigenfunctions $\chi_j^{sp}(\mu)$. We consider $\mathcal{D} = [1, 1] \times [1, 20] \times [-0.1, 0.1] \times [-0.1, 0.1] \times [-0.1, 0.1]$, a training set $\Xi$ of size 250, and $\varepsilon = 2 \cdot 10^{-6}$. On average the port spaces $\Lambda_{\mathcal{RB}}^{n,f}(\mu)$ have had a size of about 35.5 and the maximal encountered size has been 38. In Figure 6.7(a) we plot the training

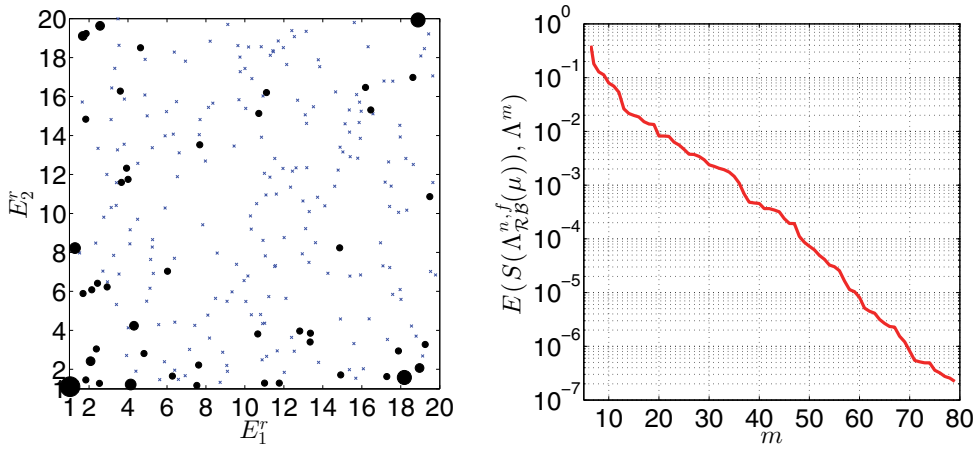


(a) $\Xi$, $\mu$ selected by greedy

(b) $E(S(\Lambda_{\mathcal{RB}}^{n,f}(\mu)), \Lambda^m)$

FIG. 6.7. (a) *The training set $\Xi \subset \mathcal{D}$ (crosses) and the parameters selected during the spectral greedy algorithm (dots).* (b) *The behavior of $E(S(\Lambda_{\mathcal{RB}}^{n,f}(\mu)), \Lambda^m)$ during the spectral greedy algorithm.*

set $\Xi$ (crosses) and indicate the parameters which are selected by the spectral greedy algorithm with dots; the size of the dots scales linearly with the number of times a parameter has been selected. First, we observe that the configurations with a small Young's modulus ratio and especially the configuration with the smallest Young's modulus ratios $E_1^r = 1.0214$, $E_2^r = 1.1085$ in $\Xi$ are selected rather often. For those configurations the spectral greedy algorithm chooses in particular higher membrane, bending, or torsional modes—modes that have the same shape as a higher lateral or vertical bending mode or torsional mode of a beam with free ends[12] (see [45]). This seems plausible, as those modes cannot be found in the port spaces of, say, the configurations $E_i^r = 20$ and $E_1^r = 10$ and $E_2^r = 13$. Note that this is consistent with the more uniform behavior of the stiffened plate, as mentioned at the beginning of this subsection. For configurations with a relatively high Young's modulus ratio, the space $\Lambda^m$ is mainly enhanced with lower membrane, bending, or torsional modes or deformations such as a simultaneous shrinking in $x_3$ and enlargement in the $x_2$-direction. Moreover, we observe a strong coincidence of the spectral modes of the configurations $E_i^r = 20$ and $E_1^r = 10$ and $E_2^r = 13$. This might explain why the spectral greedy algorithm chooses relatively few functions of port spaces $\Lambda_{\mathcal{RB}}^{n,f}(\mu)$ associated with a parameter configuration where both $E_1^r$ and $E_2^r$ lie in the interval $[8, 16]$.

Finally, we observe in Figure 6.7(b) a very rapid and exponential convergence of $E(S(\Lambda_{\mathcal{RB}}^{n,f}(\mu)), \Lambda^m)$ during the spectral greedy algorithm such that the port space $\Lambda^m$ is of a relatively small dimension of 79. This might be explained by the fact that, apart from the above-stated differences, the port spaces $\Lambda_{\mathcal{RB}}^{n,f}(\mu)$ share (albeit possibly disturbed) lower bending, membrane, and to some extent torsional modes. In particular, we observe little variation for the first nine modes. We thus infer that at least for the current numerical example a variation in the parameter affects the port spaces $\Lambda_{\mathcal{RB}}^{n,f}(\mu)$ and especially the lower spectral modes only moderately.

Next, we analyze the convergence of the relative error of the port-reduced sc

[12] Note that we use here the term membrane displacement in the sense of [8], i.e., that the respective displacement is symmetric with respect to the midsurface of the plate.

approximation. First, we compare the convergence for Legendre modes, empirical port modes, and spectral port modes for a system of two components with $E_i = E_i^r = 1$, $i = 1, 2$, $\mathbf{g} = (0, 0, 0)^T$, $u_{D,1} = (1, 1, 1)^T$, and $u_{D,2} = (0, 0, 0)^T$. The error decay for the Legendre modes is very slow and in particular much slower than that of the empirical and spectral port modes. For instance, for $m = 50$ the relative error for the Legendre modes still amounts to about 7%, while for $m = 18$ the relative error of the empirical and spectral modes has already dropped to about 0.002. The convergence for the empirical modes and the spectral modes is comparable. This is maybe due to the fact that for the ship stiffener application the boundary conditions seem to affect the solution $u(\mu)$ much more than for the solid beam, making it simpler for the pairwise training algorithm to identify modes associated with the boundary conditions. We expect that for more complex boundary conditions the spectral modes converge faster than the empirical modes.[13] This can indeed be observed for a `system 1` of two components for which we prescribe $E_i = E_i^r = 1$, $i = 1, 2$, $\mathbf{g} = (0, 0, 0)^T$, $u_{D,1} = 5\eta_6|_{\Gamma_1}/\|\eta_6|_{\Gamma_1}\|_{\Gamma_1}$, and $u_{D,2} = -2.5\eta_6|_{\Gamma_2}/\|\eta_6|_{\Gamma_2}\|_{\Gamma_2}$; note that the prescribed boundary conditions cause a rotation of the ports $\Gamma_1$ and $\Gamma_2$ in the planes of the ports but in relative opposite direction, causing a twisting of the plate. Comparing the relative approximation error for the empirical and spectral port modes in Figure 6.8(a), we observe that for the empirical modes only two port modes seem to cause a significant reduction of the error, as opposed to five for the spectral modes. This may be because the higher torsional modes that reduce the error for the spectral modes do not lie within the span of the empirical port modes.

In order to investigate the approximation behavior of the spectral modes for more complex boundary conditions, we consider a `system 2` with $E_i = 1$, $i = 1, 2$. First, we compare the convergence of the relative error $|||u(\mu) - u^m(\mu)|||_\mu / |||u(\mu)|||_\mu$ for $\mathbf{g} = (0, -0.04, 0)^T$, $u_{D,1} = 0.1\sum_{j=1}^{10} \chi_j$, $u_{D,2} = 0.1(-\chi_1 + \chi_2 - \chi_3 - \chi_4 - \chi_5 + \chi_6 + \chi_7 - \chi_8 + \chi_9 + \chi_{10})$,[14] and the Young's modulus ratios $E_i^r = 1$, $E_i^r = 20$, $i = 1, 2$, $E_1^r = 10$, $E_2^r = 13$, and $E_1^r = 1$, $E_2^r = 20$; note that we thus have $\mu \notin \Xi$ for all four parameter configurations. We observe in Figure 6.8(b) for those four parameter values a very rapid and exponential convergence. A very similar convergence is obtained for a parameter configuration $E_1^r = 9.443$, $E_2^r = 13.46$, $\mathbf{g} = (-0.04, -0.0009, -0.0434)^T$, which lies in $\Xi$ but is *not* selected by the spectral greedy algorithm, and a parameter configuration $E_1^r = 1.6796$, $E_2^r = 19.112$, $\mathbf{g} = (0.0278, 0.0852, 0.0448)^T$ that has been chosen by the spectral greedy algorithm (see Figure 6.8(b)), where we consider $u_{D,1} = 0.1(\chi_1 - \chi_2 + \chi_3 + \chi_4 - \chi_5 + \chi_6 - \chi_7 + \chi_8 + \chi_9 - \chi_{10})$ and $u_{D,2} = 0.1(-\chi_1 - \chi_2 - \chi_3 - \chi_4 + \chi_5 + \chi_6 - \chi_7 - \chi_8 + \chi_9 - \chi_{10})$. Finally, the convergence for the parameter configuration $E_1^r = 9.443$, $E_2^r = 13.46$, $\mathbf{g} = (-0.04, -0.0009, -0.0434)^T$, which is in $\Xi$, and the parameter $E_1^r = 10$, $E_2^r = 13$, $\mathbf{g} = (-0.04, -0.0009, -0.0434)^T$, which does *not* lie in $\Xi$, with the same Dirichlet boundary conditions nearly coincides. This demonstrates also for the ship stiffener application the very good approximation properties of the spectral port modes and that the spectral greedy Algorithm 4.1 is able to build a parameter-independent port space that yields a very rapid and exponential convergent sc approximation. We may also infer that although the con-

[13] Note that during the pairwise training algorithm, we prescribe for each component $u_{D,i}^l = \sum_{k=1}^{\mathcal{N}_\Gamma/3}(rL_k)/k^\gamma$ [11, 12], $i = 1, 2$, $l = 1, 2, 3$, where $r$ is a random number, $\gamma$ a smoothing parameter, and $L_k$ the Legendre-type function introduced in section 6.2. Thanks to the factor $k^{-\gamma}$, the higher Legendre modes are penalized.

[14] Note that prescribing a linear combination of the spectral basis $\{\chi_i\}_{i=1}^m$ on $\Gamma_1$ and $\Gamma_2$ does *not* imply $u(\mu)|_{\Gamma_{12}} \in \Lambda^m$.

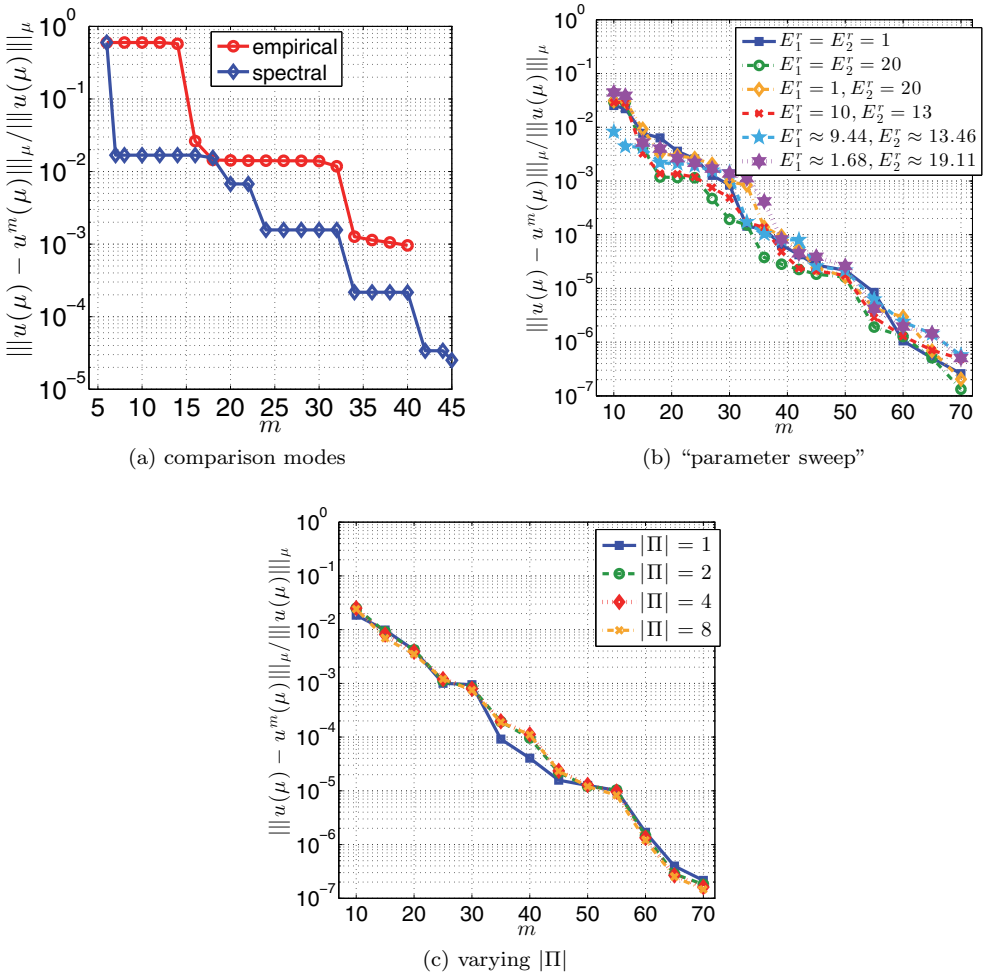


(a) comparison modes

(b) "parameter sweep"

(c) varying $|\Pi|$

FIG. 6.8. $|||u(\mu)-u^m(\mu)|||_\mu / |||u(\mu)|||_\mu$ *for the empirical and spectral port modes for* (a) `system 1`, (b) `system 2` *and varying parameters* $\mu \in \mathcal{D}$, *and* (c) `system 3` *and an increasing number of ports in the global system* $|\Pi|$.

vergence result in Theorem 4.4 only applies for parameters in $\Xi$, the convergence will not worsen for $\mu \notin \Xi$ for $\Xi$ sufficiently rich. Finally, we emphasize that in contrast to the eigenvalues of the transfer eigenvalue problem, the convergence of the sc approximation based on the port space constructed by the spectral greedy algorithm is only slightly affected by the choice of $E_i^r$.

To investigate the convergence of the relative error for an increasing number of ports $|\Pi|$ within the global system, we consider a `system 3` of $I$ components, $E_i = E_i^r = 1$, $i = 1, \ldots, I$, and $\mathbf{g} = (0, 0, 0)^T$. Similarly to the previous example, we prescribe $u_{D,1} = 0.1(\chi_1 - \chi_2 - \chi_3 + \chi_4 - \chi_5 - \chi_6 + \chi_7 - \chi_8 + \chi_9 - \chi_{10})$ and $u_{D,2} = 0.1(-\chi_1 + \chi_2 - \chi_3 - \chi_4 - \chi_5 + \chi_6 + \chi_7 - \chi_8 + \chi_9 + \chi_{10})$. We observe in Figure 6.8(c) that the convergence for $|\Pi| = 2, 4, 8$ is nearly the same and that a linear scaling in the number of ports cannot be detected.

**7. Conclusions.** We have proposed port spaces for sc approximations that are optimal in the sense of Kolmogorov [29]. To this end we have introduced a (compact)

transfer operator that acts on the space of harmonic extensions on a component pair and maps the traces on the ports on the boundary of the two-component system to the shared port. It can then be shown, similarly to [3], that the optimal port space is spanned by the lowest eigenfunctions of the transfer eigenvalue problem of the composition of the transfer operator and its adjoint. Additionally, we have introduced a spectral greedy algorithm that constructs a quasi-optimal [9] parameter-independent port space from the union of all parameter-dependent port spaces. Finally, we have proved, for certain algorithmic choices, that the spectral greedy yields, for any given tolerance and anticipated number of ports in the online system, an sc approximation which is bounded (for all parameters in a rich train set) by the prescribed tolerance. The theoretical results have been presented for exact local approximation spaces. Taking into account errors due to FE and RB approximation is the subject of future work.

The numerical experiments demonstrate an extremely rapid and exponential convergence of the eigenvalues for a simple beam of square cross-section, an I-beam with an internal crack, and a simplified ship stiffener component. Furthermore, we have observed that the spectral port spaces yield a very rapid and exponentially convergent sc approximation, also for parameters outside the train set. This rapid convergence represents a substantial improvement over singular Sturm–Liouville expansions, and also, particularly for higher accuracies, an improvement over the port spaces generated by the empirical pairwise training procedure of [11]; furthermore, and unlike the method of [11], our approach allows us to control the accuracy of the sc approximation a priori during the offline stage.

**Appendix A. Rigid body modes.** We consider the local spaces of rigid body modes

$$\mathcal{RB}_{\Omega_i} := \{a + b \times (x_1, x_2, x_3)^t,\ \ a, b \in \mathbb{R}^3,\ \ x = (x_1, x_2, x_3)^t \in \Omega_i\}, \quad i = 1, 2, \tag{A.1}$$

and for $x = (x_1, x_2, x_3)^t \in \Omega_i$, $i = 1, 2$, the following basis:

$$\begin{aligned} &\eta_1(x_1, x_2, x_3) = (1, 0, 0),\ \ \eta_2(x_1, x_2, x_3) = (0, 1, 0),\ \ \eta_3(x_1, x_2, x_3) = (0, 0, 1), \\ &\eta_4(x_1, x_2, x_3) = (x_2, -x_1, 0),\ \ \eta_5(x_1, x_2, x_3) = (x_3, 0, -x_1),\ \ \eta_6(x_1, x_2, x_3) = (0, x_3, -x_2). \end{aligned} \tag{A.2}$$

Note that since each of these modes has zero strain, the functions $\eta_1|_{\Omega_i}, \ldots, \eta_6|_{\Omega_i}$ are also a basis for the nullspace of the bilinear forms $a_i(\cdot, \cdot)$, $i = 1, 2$. This can be exploited to represent the functions in $\mathcal{RB}_{\Omega_i}$, $i = 1, 2$, by the $a$-harmonic extensions (2.10) of the restrictions of the rigid body modes to the ports, as stated in the following lemma.

LEMMA A.1. *There holds* $\mathcal{RB}_{\Omega_i} \subset \operatorname{span}\{\mathcal{L}_{i,\Gamma_i}\eta_k|_{\Gamma_i}, \mathcal{L}_{i,\Gamma_{12}}\eta_k|_{\Gamma_{12}}, k = 1, \ldots, 6\}$, $i = 1, 2$.

*Proof.* Thanks to the definition of the $a$-harmonic extensions, we have for $i = 1, 2$, $k = 1, \ldots, 6$

$$\begin{aligned} \big(\mathcal{L}_{i,\Gamma_i}\eta_k|_{\Gamma_i} + \mathcal{L}_{i,\Gamma_{12}}\eta_k|_{\Gamma_{12}}\big)|_{\Gamma_i} = \eta_k|_{\Gamma_i}, \quad \big(\mathcal{L}_{i,\Gamma_i}\eta_k|_{\Gamma_i} + \mathcal{L}_{i,\Gamma_{12}}\eta_k|_{\Gamma_{12}}\big)|_{\Gamma_{12}} = \eta_k|_{\Gamma_{12}}, \\ a_i(\eta_k, v) = a_i(\mathcal{L}_{i,\Gamma_i}\eta_k|_{\Gamma_i} + \mathcal{L}_{i,\Gamma_{12}}\eta_k|_{\Gamma_{12}}, v) = 0 \quad \forall v \in X_{i;0}. \end{aligned}$$

We consider the following problem: Find $w \in X_{i;\eta_k} := \{v \in [H^1(\Omega)]^3 : v|_{\Gamma_{12}} = \eta_k|_{\Gamma_{12}}, v|_{\Gamma_i} = \eta_k|_{\Gamma_i}\}$ such that

$$a_i(w, v) = 0 \quad \forall v \in X_{i;0}, \quad i = 1, 2. \tag{A.3}$$

This problem is well-posed thanks to Korn's inequality and therefore has a unique solution. As there holds $\eta_k|_{\Omega_i} \in X_{i;\eta_k}$, $i = 1, 2$, $k = 1, \dots, 6$, we may thus conclude that we have

$$\eta_k = \mathcal{L}_{i,\Gamma_i}\eta_k|_{\Gamma_i} + \mathcal{L}_{i,\Gamma_{12}}\eta_k|_{\Gamma_{12}} \quad \text{almost everywhere in } \Omega_i. \qquad \square$$

**Appendix B. Proofs.** First, we define an $a$-harmonic extension operator $\mathcal{E} : [H^{1/2}(\Gamma_1 \cup \Gamma_2)]^3 \to [H^1(\Omega)]^3$ of (arbitrary Dirichlet boundary) functions $\xi \in [H^{1/2}(\Gamma_1 \cup \Gamma_2)]^3$ via

$$a(\mathcal{E}\xi, v) = 0 \quad \forall v \in X_0 \qquad \text{and} \quad (\mathcal{E}\xi)|_{\Gamma_1\cup\Gamma_2} = \xi. \tag{B.1}$$

### B.1. Proofs of section 3.

LEMMA B.1. *For $w \in \mathcal{H}$ there holds $w = \mathcal{E}(w|_{\Gamma_1\cup\Gamma_2})$ almost everywhere in $\Omega$.*

*Proof.* As $w \in \mathcal{H} = \tilde{\mathcal{H}}/\mathcal{RB}$ we can write $w = \tilde{w} + w_{\mathcal{RB}}$ with $\tilde{w} \in \tilde{\mathcal{H}}$ and $w_{\mathcal{RB}} \in \mathcal{RB}$. Thanks to the linearity of the extension and the trace operator, it is sufficient to show that $\tilde{w} = \mathcal{E}(\tilde{w}|_{\Gamma_1\cup\Gamma_2})$ and $w_{\mathcal{RB}} = \mathcal{E}(w_{\mathcal{RB}}|_{\Gamma_1\cup\Gamma_2})$ almost everywhere in $\Omega$. From the definition of the space $\tilde{\mathcal{H}}$ and properties of the trace operator and the extension operator $\mathcal{E}$, we infer that $\mathcal{E}(\tilde{w}|_{\Gamma_1\cup\Gamma_2}) = \mathcal{E}((\mathcal{E}\tilde{\xi})|_{\Gamma_1\cup\Gamma_2}) = \mathcal{E}\tilde{\xi}$, where $\tilde{w}|_{\Gamma_i} = \tilde{\xi}|_{\Gamma_i}$, $i = 1, 2$, for $\tilde{\xi} \in [H^{1/2}(\Gamma_1 \cup \Gamma_2)]^3$. We may thus infer that $\tilde{w} = \mathcal{E}(\tilde{w}|_{\Gamma_1\cup\Gamma_2})$ almost everywhere in $\Omega$. Next, we consider the problem

$$a(\mathcal{E}(w_{\mathcal{RB}}|_{\Gamma_1\cup\Gamma_2}), v) = 0 \quad \forall v \in X_0 \qquad \text{and} \quad \big(\mathcal{E}w_{\mathcal{RB}}|_{\Gamma_1\cup\Gamma_2}\big)|_{\Gamma_i} = w_{\mathcal{RB}}|_{\Gamma_i}, \quad i = 1, 2. \tag{B.2}$$

First, we note that $w_{\mathcal{RB}}$ lies in the kernel of the bilinear form $a(\cdot, \cdot)$ and thus satisfies (B.2). As (B.2) is well-posed thanks to Korn's inequality and the solution of (B.2) is thus unique, we conclude that $w_{\mathcal{RB}} = \mathcal{E}w_{\mathcal{RB}}|_{\Gamma_1\cup\Gamma_2}$. $\square$

*Proof of Lemma* 3.4. Define a cut-off function $\zeta \in C^1(\Omega)$ with the following properties: $0 \le \zeta \le 1$, $\zeta \equiv 1$ on $\Omega^*$ and $\zeta \equiv 0$ on $\Omega\backslash\Omega^{**}$, and $\max_{1\le i\le 3} |\frac{\partial\zeta}{\partial x_i}| \le \frac{1}{\varrho}$. Choosing $v = w\zeta^2$ as a test function in (3.7) yields $\int_\Omega E(x)\frac{\partial w^i}{\partial x_j}C_{ijkl}\frac{\partial(w^k\zeta^2)}{\partial x_l}dx = 0$, and therefore

$$\begin{aligned}\int_\Omega E(x)\frac{\partial w^i}{\partial x_j}C_{ijkl}\frac{\partial w^k}{\partial x_l}\zeta^2 dx &= -2\int_\Omega E(x)\frac{\partial w^i}{\partial x_j}C_{ijkl}\frac{\partial\zeta}{\partial x_l}\zeta w^k dx \\ &\le \left(\int_\Omega E(x)\frac{\partial w^i}{\partial x_j}C_{ijkl}\frac{\partial w^k}{\partial x_l}\zeta^2 dx\right)^{1/2}\left(4\int_\Omega E(x)\frac{\partial\zeta}{\partial x_j}C_{ijkl}\frac{\partial\zeta}{\partial x_l}w^i w^k dx\right)^{1/2}.\end{aligned}$$

Exploiting the properties of $\zeta$, the definition of the stiffness tensor, and the definition of $E$ yields

$$\begin{aligned}E_0\int_{\Omega^*}\frac{\partial w^i}{\partial x_j}C_{ijkl}\frac{\partial w^k}{\partial x_l}dx &\le \int_\Omega E(x)\frac{\partial w^i}{\partial x_j}C_{ijkl}\frac{\partial w^k}{\partial x_l}\zeta^2 dx \\ &\le \|E\|_{[L^\infty(\Omega)]^3}\frac{12}{\varrho^2}\frac{1-\nu}{(1+\nu)(1-2\nu)}\|w\|^2_{[L^2(\Omega^{**}\backslash\Omega^*)]^3}. \qquad \square\end{aligned}$$

PROPOSITION B.2. *The operator $P : \mathcal{H}_{\Gamma_1\cup\Gamma_2} \to \mathcal{H}_{\Gamma_{12}}$ as defined in* (3.6) *is compact.*

*Proof.* Let $w_m$ be a sequence in $\mathcal{H}$ which satisfies $\|w_m|_{\Gamma_1\cup\Gamma_2}\|_{\Gamma_1}+\|w_m|_{\Gamma_1\cup\Gamma_2}\|_{\Gamma_2} \leq C$ for some positive constant $C<\infty$. Thanks to the definition of the $\|\cdot\|_\Gamma$-norm we thus have $\|w_m|_{\Gamma_1\cup\Gamma_2}\|_{[H^{1/2}(\Gamma_1\cup\Gamma_2)]^3} \leq C$, where we allow the constant $C$ to change within this proof. Employing the continuity of the extension operator $\mathcal{E}$ [30], we thus obtain that the sequence $\mathcal{E}(w_m|_{\Gamma_1\cup\Gamma_2})$ is bounded with respect to the $X$-norm. From Lemma B.1 we infer that also $w_m \in \mathcal{H}$ is bounded with respect to the $X$-norm and that we therefore may apply Korn's inequality in the quotient space $\mathcal{H}$ to deduce that $\|w_m\|_{[H^1(\Omega)]^3} \leq C\|w_m\|_X$. The Rellich compactness theorem then yields that the sequence $w_m$ is bounded with respect to the $L^2$-norm on $\Omega$ and has a subsequence $w_{m_n}$ which converges strongly in $[L^2(\Omega)]^3$. Moreover, as the whole sequence $w_m$ is bounded with respect to the $X$-norm, we have that the subsequence $w_{m_n}$ also converges weakly in $[H^1(\Omega)]^3$ with respect to the $X$-norm to a limit $w \in [H^1(\Omega)]^3$. From Lemma B.1 and the Lax–Milgram lemma, we infer that $w \in \mathcal{H}$.

Next, we introduce the subdomains $\Omega^* \subsetneq \Omega^{**} \subsetneq \Omega_2$ with $\partial\Omega^* \cap \Gamma_{12} = \Gamma_{12}$ and $\operatorname{dist}(\partial\Omega^* \setminus \partial\Omega_2, \partial\Omega^{**} \setminus \partial\Omega_2) > \varrho > 0$. Thanks to Lemma B.1 the sequence $e_{m_n} := (w_{m_n} - w)$ satisfies (3.7), and we may apply Lemma 3.4 to $e_{m_n} \in \mathcal{H}$ to infer that

$$\int_{\Omega^*} \frac{\partial e^i_{m_n}}{\partial x_j} C_{ijkl} \frac{\partial e^k_{m_n}}{\partial x_l} dx + \|e_{m_n}\|^2_{[L^2(\Omega^*)]^3} \leq C\|e_{m_n}\|^2_{[L^2(\Omega)]^3}.$$

This allows us to make use of Korn's inequality in $[H^1(\Omega^*)]^3$ and to conclude that

$$\|e_{m_n}\|^2_{[H^1(\Omega^*)]^3} \leq C \int_{\Omega^*} \frac{\partial e^i_{m_n}}{\partial x_j} C_{ijkl} \frac{\partial e^k_{m_n}}{\partial x_l} dx + \|e_{m_n}\|^2_{[L^2(\Omega^*)]^3}.$$

From the trace theorem we infer that $\|e_{m_n}|_{\Gamma_{12}}\|_{[H^{1/2}(\Gamma_{12})]^3} \leq C\|e_{m_n}\|_{[H^1(\Omega^*)]^3}$. Thanks to the continuity of the extension operator $\mathcal{L}_{i,\Gamma_{12}}$ [30], we obtain $\|\mathcal{L}_{i,\Gamma_{12}}(e_{m_n}|_{\Gamma_{12}})\|_{X_i} \leq C\|e_{m_n}|_{\Gamma_{12}}\|_{[H^{1/2}(\Gamma_{12})]^3}$, $i=1,2$, and thus $\|e_{m_n}|_{\Gamma_{12}}\|_{\Gamma_{12}} \leq C\|e_{m_n}|_{\Gamma_{12}}\|_{[H^{1/2}(\Gamma_{12})]^3}$. Combining these estimates results in $\|w_{m_n}|_{\Gamma_{12}} - w|_{\Gamma_{12}}\|_{\Gamma_{12}} \leq C\|w_{m_n} - w\|_{[L^2(\Omega)]^3}$. Hence the subsequence $w_{m_n}|_{\Gamma_{12}}$ converges strongly in $\mathcal{H}_{\Gamma_{12}}$ to a limit $w|_{\Gamma_{12}} \in \mathcal{H}_{\Gamma_{12}}$, which was to be proven. ∎

*Proof of Proposition* 3.8. First, we assume that $u \notin \mathcal{RB}_\Omega$, because otherwise we exploit Lemma A.1 to conclude that $\|u-u^n\|_X = 0$ and the estimate (3.24) is vacuously true.

Next, we assume without loss of generality that the orthogonal projections of $\eta_j|_{\Gamma_{12}}$, $j=1,\dots,6$, on $\Lambda^n$ in (3.12) and $\Phi^f|_{\Gamma_{12}}$ on $\Lambda^n_{\mathcal{RB}}$ in (3.16) are zero. For the sake of clarity we denote in this proof by $\Phi_j^{\mathcal{RB}}$ the $a$-harmonic extensions (see (2.14)) of $\chi_j^{\mathcal{RB}}$, $j=1,\dots,6$, and by $\Phi_k^{sp}$ the $a$-harmonic extensions of the functions $\chi_k^{sp}$, $k=1,\dots,n$, defined in (3.10). Next, we define the function $u^n_{sp}$ as

$$u^n_{sp} := \sum_{i=1}^{2} \big(b_i^f + \mathcal{L}_{i,\Gamma_i} u_{D,i}\big) + \sum_{j=1}^{6} u^{\mathcal{RB}}_{sp,j} \Phi_j^{\mathcal{RB}} + \sum_{k=1}^{n} u^n_{sp,k} \Phi_k^{sp} + \Phi^f, \tag{B.3}$$

where the coefficient of $\Phi^f$ has been chosen as $\equiv 1$ and the coefficients $u^{\mathcal{RB}}_{sp,j}, u^n_{sp,k} \in \mathbb{R}$, $j=1,\dots,6$, $k=1,\dots,n$, will be specified below. Note that $u^n_{sp}$ lies in the same space as $u^n$ (to this end, compare (B.3) with (3.19)). As indicated above, we may then apply Céa's lemma to infer

$$\|u-u^n\|_X \leq \|u-u^n_{sp}\|_X. \tag{B.4}$$

Recall that we can write $u = u^f + \tilde{u}^0$, where $u^f$ and $\tilde{u}^0$ solve (3.14), and that there holds $u^f = b^f + \Phi^f$. Similar to (2.9) and by exploiting $(\mathcal{L}_{i,\Gamma_i}(\mu_i)u_{D,i})|_{\Gamma_{12}} = 0$, $i = 1, 2$, we can then represent $u$ in the following way:

$$u = \Phi^f + \sum_{i=1}^{2} \big(b_i^f + \mathcal{L}_{i,\Gamma_i} u_{D,i} + \mathcal{L}_{i,\Gamma_{12}}(\tilde{u}^0|_{\Gamma_{12}})\big). \tag{B.5}$$

We thus obtain

$$\|u - u_{sp}^n\|_X^2 = \left\| \sum_{i=1}^{2} \mathcal{L}_{i,\Gamma_{12}}(\tilde{u}^0|_{\Gamma_{12}}) - \sum_{j=1}^{6} u_{sp,j}^{\mathcal{RB}} \Phi_j^{\mathcal{RB}} - \sum_{k=1}^{n} u_{sp,k}^n \Phi_k^{sp} \right\|_X^2. \tag{B.6}$$

Observe that the representations of the right-hand side have canceled. Next, we address the representations of the rigid body modes. To that end we define $u_{\mathcal{RB}} := \arg\inf_{v \in \mathcal{RB}_\Omega} \|\tilde{u}^0 - v\|_{[H^1(\Omega)]^3}$ for $\tilde{u}^0 \in \tilde{\mathcal{H}}$ and obtain that

$$u^0 := \tilde{u}^0 - u_{\mathcal{RB}} \in \mathcal{H}. \tag{B.7}$$

Then we choose the coefficients $u_{sp,j}^{\mathcal{RB}}$, $j = 1, \dots, 6$, in (B.3) such that there holds

$$\sum_{j=1}^{6} u_{sp,j}^{\mathcal{RB}} \chi_j^{\mathcal{RB}} = u_{\mathcal{RB}}|_{\Gamma_{12}}.$$

This allows us to conclude that

$$\begin{aligned}
\|u - u_{sp}^n\|_X^2 &= \left\| \sum_{i=1}^{2} \mathcal{L}_{i,\Gamma_{12}}(\tilde{u}^0|_{\Gamma_{12}}) - \sum_{j=1}^{6} u_{sp,j}^{\mathcal{RB}} \Phi_j^{\mathcal{RB}} - \sum_{k=1}^{n} u_{sp,k}^n \Phi_k^{sp} \right\|_X^2 \\
&= \left\| \sum_{i=1}^{2} \mathcal{L}_{i,\Gamma_{12}} \left( \tilde{u}^0|_{\Gamma_{12}} - \sum_{j=1}^{6} u_{sp,j}^{\mathcal{RB}} \chi_j^{\mathcal{RB}} - \sum_{k=1}^{n} u_{sp,k}^n \chi_k^{sp} \right) \right\|_X^2 \\
&= \left\| \sum_{i=1}^{2} \mathcal{L}_{i,\Gamma_{12}} \left( \tilde{u}^0|_{\Gamma_{12}} - u_{\mathcal{RB}}|_{\Gamma_{12}} - \sum_{k=1}^{n} u_{sp,k}^n \chi_k^{sp} \right) \right\|_X^2 \\
&= \sum_{i=1}^{2} \left\| \mathcal{L}_{i,\Gamma_{12}} \left( \tilde{u}^0|_{\Gamma_{12}} - u_{\mathcal{RB}}|_{\Gamma_{12}} - \sum_{k=1}^{n} u_{sp,k}^n \chi_k^{sp} \right) \right\|_{X_i}^2 \\
&= \sum_{i=1}^{2} \left\| \mathcal{L}_{i,\Gamma_{12}} \left( u^0|_{\Gamma_{12}} - \sum_{k=1}^{n} u_{sp,k}^n \chi_k^{sp} \right) \right\|_{X_i}^2.
\end{aligned}$$

By exploiting the definition of the inner product $(\cdot,\cdot)_{\Gamma_{12}}$ in (2.13) and the definition of the transfer operator in (3.6), we arrive at

$$\|u - u_{sp}^n\|_X^2 = \left\| u^0|_{\Gamma_{12}} - \sum_{k=1}^{n} u_{sp,k}^n \chi_k^{sp} \right\|_{\Gamma_{12}}^2 = \left\| P(u^0|_{\Gamma_1 \cup \Gamma_2}) - \sum_{k=1}^{n} u_{sp,k}^n \chi_k^{sp} \right\|_{\Gamma_{12}}^2. \tag{B.8}$$

Comparing the last term in (B.8) with (3.11) motivates us to choose $\sum_{k=1}^{n} u_{sp,k}^n \chi_k^{sp}$ as the best approximation of $P(u^0|_{\Gamma_1 \cup \Gamma_2})$ in $\Lambda^n$, that is, to define the coefficients as

$u^n_{sp,k} := (\, u^0|_{\Gamma_1\cup\Gamma_2}\,, \varphi_k|_{\Gamma_1\cup\Gamma_2})_{\Gamma_1\cup\Gamma_2}$, $k = 1,\dots,n$, where the eigenfunctions $\varphi_k$ have been introduced in Proposition 3.5. We may thus conclude

$$\|u - u^n\|_X \le \sqrt{\lambda_{n+1}}\, \|u^0|_{\Gamma_1\cup\Gamma_2}\|_{\Gamma_1\cup\Gamma_2}. \tag{B.9}$$

Exploiting $\|u^0|_{\Gamma_1\cup\Gamma_2}\|_{\Gamma_1\cup\Gamma_2} \le C_1(\Omega)\,\|u\|_X$ (for the proof, see Lemma B.3) yields the assertion. ∎

LEMMA B.3. *Let $u$ be the solution of (2.3), and let $u^0$ be defined as in (B.7). Then there holds*

$$\|u^0|_{\Gamma_1\cup\Gamma_2}\|_{\Gamma_1\cup\Gamma_2} \le C_1(\Omega)\|u\|_X, \tag{B.10}$$

*where the constant $C_1(\Omega)$ depends on neither $u$ nor $u^n$.*

*Proof.* As $u^0 \in \mathcal{H}$ we may apply Lemma B.1 to infer that $u^0 = \mathcal{E}u^0|_{\Gamma_1\cup\Gamma_2}$, where $\mathcal{E}$ has been defined in (B.1). Thanks to the Lax–Milgram lemma, we thus obtain

$$\|u^0\|_X = a(u^0,u^0) = \min\left\{a(v,v)\,:\, v\in[H^1(\Omega)]^3, v|_{\Gamma_1\cup\Gamma_2} = u^0|_{\Gamma_1\cup\Gamma_2}\right\}.$$

Therefore, there holds

$$\|u^0\|_X \le \|v\|_X \text{ for all functions } v\in[H^1(\Omega)]^3 \text{ that satisfy } u^0|_{\Gamma_1\cup\Gamma_2} = v|_{\Gamma_1\cup\Gamma_2}. \tag{B.11}$$

Recall that we can write $u = u^f + \tilde{u}^0 = u^f + u^0 + u_{\mathcal{RB}}$, where $u^f \in X_0 = \{v \in [H^1(\Omega)]^3 \,:\, v = 0 \text{ on } \Gamma_1,\Gamma_2\}$, yielding $(u - u_{\mathcal{RB}})|_{\Gamma_1\cup\Gamma_2} = u^0|_{\Gamma_1\cup\Gamma_2}$. We may thus apply (B.11) to conclude $\|u^0\|_X \le \|u - u_{\mathcal{RB}}\|_X$. As $u_{\mathcal{RB}}$ has zero strain (see Appendix A) and thus satisfies $\|u_{\mathcal{RB}}\|_X = 0$, we infer $\|u^0\|_X \le \|u\|_X$ and thus

$$\frac{\|u^0|_{\Gamma_1\cup\Gamma_2}\|_{\Gamma_1\cup\Gamma_2}}{\|u\|_X} \le \frac{\|u^0|_{\Gamma_1\cup\Gamma_2}\|_{\Gamma_1\cup\Gamma_2}}{\|u^0\|_X} \le C_1(\Omega).$$

Note that the independence of the constant $C_1(\Omega)$ on $u$ follows from the trace theorem and Korn's inequality for the quotient space $\mathcal{H}$. ∎

### B.2. Proofs of section 4.

*Proof of Proposition* 4.2. The assertion is obtained by following along the lines of the proof of Proposition 3.8 and exploiting that, thanks to the Lax–Milgram lemma and the corresponding energy minimizing principle similar to (B.11), we have that

$$\begin{aligned}\left|\!\left|\!\left| \mathcal{L}_{i,\Gamma_{12}}(\mu_i)\left(u^0(\mu)|_{\Gamma_{12}} - \sum_{k=1}^n u^n_{sp,k}\chi^{sp}_k(\mu)\right)\right|\!\right|\!\right|_{\mu,i} \\ \le \left|\!\left|\!\left| \mathcal{L}_{i,\Gamma_{12}}(\bar{\mu}_i)\left(u^0(\mu)|_{\Gamma_{12}} - \sum_{k=1}^n u^n_{sp,k}\chi^{sp}_k(\mu)\right)\right|\!\right|\!\right|_{\mu,i}.\end{aligned} \tag{B.12}$$

∎

*Proof of Theorem* 4.4. Let $\mu \in \Xi$ be fixed but arbitrary. Recall that we can assume $u(\mu) \notin \mathcal{RB}_\Omega$ and that we can write

$$u(\mu) = \Phi^f(\mu) + \sum_{i=1}^2 \big(b^f_i(\mu_i) + \mathcal{L}_{i,\Gamma_i}(\mu_i)u_{D,i} + \mathcal{L}_{i,\Gamma_{12}}(\mu_i)(\tilde{u}^0(\mu)|_{\Gamma_{12}})\big),$$

where $\Phi^f(\mu)$ is the $a$-harmonic extension of $\chi^f(\mu)$ and $\tilde{u}^0 \in \tilde{\mathcal{H}}(\mu)$. For details, we refer the reader to the proof of Proposition 3.8. Again, we define $u_{\mathcal{RB}}(\mu) :=$

$\arg\inf_{v\in\mathcal{RB}_\Omega}\|\tilde{u}^0(\mu)-v\|_{[H^1(\Omega)]^3}$ and obtain $u^0(\mu):=\tilde{u}^0(\mu)-u_{\mathcal{RB}}(\mu)\in\mathcal{H}(\mu)$. Next, we introduce the auxiliary function

$$\hat{u}^m(\mu):=\sum_{i=1}^{2}\big(b_i^f(\mu_i)+\mathcal{L}_{i,\Gamma_i}(\mu_i)u_{D,i}\big)+\sum_{k=1}^{m}\hat{u}_k^m(\mu)\Phi_k(\mu)+\sum_{k=1}^{6}\hat{u}_k^{\mathcal{RB}}(\mu)\Phi_k(\mu), \tag{B.13}$$

recalling that $\{\chi_1,\dots,\chi_6\}$ are obtained by orthonormalizing a basis for the rigid body modes restricted to $\Gamma_{12}$. The coefficients $\hat{u}_k^{\mathcal{RB}}(\mu)$, $k=1,\dots,6$, are thus defined such that they satisfy $\big(\sum_{k=1}^{6}\hat{u}_k^{\mathcal{RB}}(\mu)\Phi_k(\mu)\big)|_{\Gamma_{12}}=u_{\mathcal{RB}}(\mu)|_{\Gamma_{12}}$. The coefficients $\hat{u}_k^m(\mu)$, $k=1,\dots,m$, will be specified later. We also introduce again a spectral approximation,

$$\hat{u}_{sp}^n(\mu):=\Phi^f(\mu)+\sum_{k=1}^{n}(u^0(\mu)|_{\Gamma_1\cup\Gamma_2},\varphi_k(\mu)|_{\Gamma_1\cup\Gamma_2})_{\Gamma_1\cup\Gamma_2}\Phi_k^{sp}(\mu),$$

and shorten notation by setting

$$u_{sp,k}^n(\mu):=(u^0(\mu)|_{\Gamma_1\cup\Gamma_2},\varphi_k(\mu)|_{\Gamma_1\cup\Gamma_2})_{\Gamma_1\cup\Gamma_2}. \tag{B.14}$$

Proceeding similarly as in the proof of Proposition 3.8, we obtain

$$\begin{aligned}&|||u(\mu)-u^m(\mu)|||_\mu\le|||u(\mu)-\hat{u}^m(\mu)|||_\mu\\&\le\left|\left|\left|\sum_{i=1}^{2}\mathcal{L}_{i,\Gamma_{12}}(\mu_i)(u^0(\mu)|_{\Gamma_{12}})+\Phi^f(\mu)-\hat{u}_{sp}^n(\mu)\right|\right|\right|_\mu+\left|\left|\left|\hat{u}_{sp}^n(\mu)-\sum_{k=1}^{m}\hat{u}_k^m(\mu)\Phi_k(\mu)\right|\right|\right|_\mu.\end{aligned} \tag{B.15}$$

The first term in (B.15) can be treated as in the proof of Proposition 3.8, and we obtain

$$|||u(\mu)-u^m(\mu)|||_\mu\le c(\mu,\bar{\mu})\sqrt{\lambda_{n+1}(\mu)}\|u^0(\mu)|_{\Gamma_1\cup\Gamma_2}\|_{\Gamma_1\cup\Gamma_2}+\left|\left|\left|\hat{u}_{sp}^n(\mu)-\sum_{k=1}^{m}\hat{u}_k^m(\mu)\Phi_k(\mu)\right|\right|\right|_\mu.$$

We recall that within the spectral greedy Algorithm 4.1 for all $\mu\in\Xi$ the spaces $\Lambda_{\mathcal{RB}}^{n,f}(\mu)$ are computed such that there holds $c(\mu,\bar{\mu})C_1(\Omega,\mu)\sqrt{\lambda_{n+1}(\mu)}\le(1-\frac{q}{p})\varepsilon$. We may thus conclude

$$|||u(\mu)-u^m(\mu)|||_\mu\le\left(1-\frac{q}{p}\right)\varepsilon|||u(\mu)|||_\mu+\left|\left|\left|\hat{u}_{sp}^n(\mu)-\sum_{k=1}^{m}\hat{u}_k^m(\mu)\Phi_k(\mu)\right|\right|\right|_\mu. \tag{B.16}$$

Exploiting the definition of $\Phi_k(\mu)$ in (4.5), and the energy minimizing property of $\mathcal{L}_{i,\Gamma}(\mu_i)$ as in (B.12), we may estimate the last term in (B.15) as follows:

$$\left|\left|\left|\hat{u}_{sp}^n(\mu)-\sum_{k=1}^{m}\hat{u}_k^m(\mu)\Phi_k(\mu)\right|\right|\right|_\mu^2\le c(\mu,\bar{\mu})^2\left\|\hat{u}_{sp}^n(\mu)|_{\Gamma_{12}}-\sum_{k=1}^{m}\hat{u}_k^m(\mu)\chi_k\right\|_{\Gamma_{12}}^2.$$

Note that $\hat{u}_{sp}^n(\mu)|_{\Gamma_{12}}=\chi^f(\mu)+\sum_{k=1}^{n}u_{sp,k}^n(\mu)\chi_l^{sp}(\mu)\in\Lambda_{\mathcal{RB}}^{n,f}(\mu)$, where $u_{sp,k}^n(\mu)$ has been defined in (B.14). Recall that the spectral greedy Algorithm 4.1 ensures that the space $\Lambda^m$ is constructed such that we have

$$\begin{aligned}\max_{\mu\in\Xi}E(S(\Lambda_{\mathcal{RB}}^{n,f}(\mu)),\Lambda^m)&=\max_{\mu\in\Xi}\left\{\sup_{\rho\in\Lambda_{\mathcal{RB}}^{n,f}(\mu)}\inf_{\zeta\in\Lambda^m}\frac{\|\rho-\zeta\|_{\Gamma_{12}}}{\|\rho\|_{\Lambda_{\mathcal{RB}}^{n,f}(\mu)}}\right\}\\&\le\frac{\varepsilon}{(p-q)\varepsilon+pC_2(\Omega,\mu)c(\mu,\bar{\mu})}.\end{aligned}$$

Choosing $\sum_{k=1}^m \hat{u}_k^m(\mu)\chi_k$ as the orthogonal projection of $\hat{u}_{sp}^n(\mu)|_{\Gamma_{12}}$ on the space $\Lambda^m$ and thus defining the coefficients as $\hat{u}_k^m(\mu) := (\hat{u}_{sp}^n(\mu)|_{\Gamma_{12}}, \chi_k)_{\Gamma_{12}}$, $k = 1, \dots, m$, allows us to infer

(B.17)
$$\left|\!\left|\!\left| \hat{u}_{sp}^n(\mu) - \sum_{k=1}^m \hat{u}_k^m(\mu)\Phi_k(\mu) \right|\!\right|\!\right|_\mu \le \frac{\varepsilon c(\mu,\bar{\mu})}{(p-q)\varepsilon + pC_2(\Omega,\mu)c(\mu,\bar{\mu})} \|\hat{u}_{sp}^n(\mu)|_{\Gamma_{12}}\|_{\Lambda^{n,f}_{\mathcal{RB}}(\mu)}.$$

Thanks to inequalities (4.16) and (B.16), it thus remains to prove that

$$\frac{\varepsilon c(\mu,\bar{\mu})\theta(\mu)}{(p-q)\varepsilon + pC_2(\Omega,\mu)c(\mu,\bar{\mu})} \|\hat{u}_{sp}^n(\mu)|_{\Gamma_{12}}\|_{\Gamma_{12}} \le \frac{q}{p}\,\varepsilon\, |\!|\!| u(\mu) |\!|\!|_\mu, \tag{B.18}$$

where $\theta(\mu)$ has been defined in (4.16). Thanks to (3.11) we have

$$\begin{aligned}\|\hat{u}_{sp}^n(\mu)|_{\Gamma_{12}}\|_{\Gamma_{12}} &\le \|\hat{u}_{sp}^n(\mu)|_{\Gamma_{12}} - u^0(\mu)|_{\Gamma_{12}} - \chi^f(\mu)\|_{\Gamma_{12}} + \|u^0(\mu)|_{\Gamma_{12}}\|_{\Gamma_{12}} + \|\chi^f(\mu)\|_{\Gamma_{12}} \\ &\le \sqrt{\lambda_{n+1}(\mu)}\|u^0(\mu)|_{\Gamma_1\cup\Gamma_2}\|_{\Gamma_1\cup\Gamma_2} + \|u^0(\mu)|_{\Gamma_{12}}\|_{\Gamma_{12}} + \|\chi^f(\mu)\|_{\Gamma_{12}}.\end{aligned}$$

Exploiting that $a(\tilde{u}^0(\mu), u^f(\mu); \mu) = 0$ and thus $|\!|\!| u(\mu) |\!|\!|_\mu \ge |\!|\!| u^f(\mu) |\!|\!|_\mu$ and $|\!|\!| u(\mu) |\!|\!|_\mu \ge |\!|\!| \tilde{u}^0(\mu) |\!|\!|_\mu = |\!|\!| u^0(\mu) |\!|\!|_\mu$ (see the supplementary materials for a proof), we obtain

(B.19)
$$\frac{c(\mu,\bar{\mu})\theta(\mu)\|\hat{u}_{sp}^n(\mu)|_{\Gamma_{12}}\|_{\Gamma_{12}}}{|\!|\!| u(\mu) |\!|\!|_\mu} \le \frac{\theta(\mu)}{p}\left( (p-q)\varepsilon + pc(\mu,\bar{\mu}) \left\{ \frac{\|\chi^f\|_{\Gamma_{12}}}{|\!|\!| u^f(\mu) |\!|\!|_\mu} + \frac{\|u^0(\mu)|_{\Gamma_{12}}\|_{\Gamma_{12}}}{|\!|\!| u^0(\mu) |\!|\!|_\mu} \right\} \right).$$

Using the assumption $p > q \ge \max_{\mu\in\Xi}\theta(\mu)$ and exploiting that

$$\left\{ \frac{\|\chi^f\|_{\Gamma_{12}}}{|\!|\!| u^f(\mu) |\!|\!|_\mu} + \frac{\|u^0(\mu)|_{\Gamma_{12}}\|_{\Gamma_{12}}}{|\!|\!| u^0(\mu) |\!|\!|_\mu} \right\} \le C_2(\Omega,\mu)$$

with a constant $C_2(\Omega,\mu)$ that does not depend on $u(\mu)$ (see Lemma B.4) yields (B.18) and thus the assertion. ∎

LEMMA B.4. *Let $u^f(\mu) \in X_0$ and $\tilde{u}^0(\mu) \in X$ be the solutions of*

$$a(u^f(\mu), v; \mu) = f(v;\mu) \quad \forall v \in X_0 \quad \textit{and} \quad a(\tilde{u}^0(\mu), v; \mu) = 0 \quad \forall v \in X_0, \tag{B.20}$$

*and recall $u^0(\mu) = \tilde{u}^0(\mu) - \arg\inf_{v\in\mathcal{RB}_\Omega} \|\tilde{u}^0(\mu) - v\|_{[H^1(\Omega)]^3}$. Then there holds*

$$\left\{ \frac{\|\chi^f\|_{\Gamma_{12}}}{|\!|\!| u^f(\mu) |\!|\!|_\mu} + \frac{\|u^0(\mu)|_{\Gamma_{12}}\|_{\Gamma_{12}}}{|\!|\!| u^0(\mu) |\!|\!|_\mu} \right\} \le C_2(\Omega,\mu)$$

*with a constant $C_2(\Omega,\mu)$ that does not depend on $u(\mu)$.*

*Proof.* The definition of the norm $\|\cdot\|_{\Gamma_{12}}$, an energy minimizing argument similar to (B.12), the definition of $\Phi^f(\mu)$, and Lemma 4.1 yield

$$\begin{aligned}\|\chi^f(\mu)\|_{\Gamma_{12}}^2 &= \sum_{i=1}^2 |\!|\!| \mathcal{L}_{i,\Gamma_{12}}(\bar{\mu}_i)\chi^f(\mu_i) |\!|\!|_i^2 \le \sum_{i=1}^2 |\!|\!| \mathcal{L}_{i,\Gamma_{12}}(\mu_i)\chi^f(\mu_i) |\!|\!|_i^2 \\ &= |\!|\!| \Phi^f(\mu) |\!|\!|^2 \le |\!|\!| \Phi^f(\mu) |\!|\!|_\mu^2.\end{aligned}$$

Recall that we have $u^f(\mu) = \Phi^f(\mu) + \sum_{i=1}^2 b_i^f(\mu_i)$. Thanks to the the definition of $\mathcal{L}_{i,\Gamma_{12}}(\mu_i)$ in (4.4) and the fact that $b_i^f(\mu_i) \in X_{i;0}$, there holds $a_i(\Phi^f(\mu)|_{\Omega_i}, b_i^f(\mu_i); \mu_i) = 0$, $i = 1, 2$. We can thus infer that there holds $|||u^f(\mu)|_{\Omega_i}|||_{\mu,i}^2 = |||\Phi^f(\mu)|_{\Omega_i}|||_{\mu,i}^2 + |||b_i^f(\mu_i)|||_{\mu,i}^2$, and as a consequence $|||\Phi^f(\mu)|||_\mu \leq |||u^f(\mu)|||_\mu$ and $(\|\chi^f(\mu)\|_{\Gamma_{12}}^2 / |||u^f(\mu)|||_\mu) \leq 1$.

To estimate the term $\|u^0(\mu)|_{\Gamma_{12}}\|_{\Gamma_{12}} / |||u^0(\mu)|||_\mu$ we first introduce the functions

$$L_{i,\Gamma_{12}} := \left[\sum_{k=1}^3 \mathcal{L}_{i,\Gamma_{12}}(\bar{\mu}_i)\eta_k|_{\Gamma_{12}}\right] u^0(\mu), \quad i = 1, 2.$$

Note that, thanks to $(\sum_{k=1}^3 \eta_k|_{\Gamma_{12}}) = (1, 1, 1)^T$ and the definition of $\mathcal{L}_{i,\Gamma_{12}}(\mu_i)$ in (4.4), there hold $L_{i,\Gamma_{12}}|_{\Gamma_{12}} = \left(\mathcal{L}_{i,\Gamma_{12}}(\bar{\mu}_i)(u^0(\mu)|_{\Gamma_{12}})\right)|_{\Gamma_{12}}$ and $L_{i,\Gamma_{12}}|_{\Gamma_i} = \left(\mathcal{L}_{i,\Gamma_{12}}(\bar{\mu}_i)(u^0(\mu)|_{\Gamma_{12}})\right)|_{\Gamma_i} = 0$. Similarly as in the proof of Lemma B.3, we can thus exploit the energy minimizing property of $\mathcal{L}_{i,\Gamma_{12}}(\bar{\mu}_i)(u^0(\mu)|_{\Gamma_{12}})$ thanks to the Lax–Milgram lemma:

$$\|u^0(\mu)|_{\Gamma_{12}}\|_{\Gamma_{12}}^2 = \sum_{i=1}^2 |||\mathcal{L}_{i,\Gamma_{12}}(\bar{\mu}_i)(u^0(\mu)|_{\Gamma_{12}})|||_i^2 \leq \sum_{i=1}^2 |||L_{i,\Gamma_{12}}|||_i^2.$$

Exploiting that $\left\|\left(\sum_{k=1}^3 \mathcal{L}_{i,\Gamma_{12}}(\bar{\mu}_i)\eta_k|_{\Gamma_{12}}\right)^k\right\|_{L^\infty(\Omega_i)} \leq 1$, $i = 1, 2$, where the superscript $k$ denotes the $k$th component of the vector field, and using the product rule for differentiation, Hölder's inequality, and Young's inequality, we may now continue with our estimate as follows:

$$\|u^0(\mu)|_{\Gamma_{12}}\|_{\Gamma_{12}}^2 \leq 2\left(|||u^0(\mu)|||^2 + c_\Omega c_\nu \|u^0(\mu)\|_{[L^2(\Omega)]^3}^2\right),$$

where $c_\Omega := \max_{i=1,2}\max_{j=1,2,3} |(\sum_{k=1}^3 \mathcal{L}_{i,\Gamma_{12}}(\bar{\mu}_i)\eta_k|_{\Gamma_{12}})^j|_{W^{1,\infty}(\Omega_i)}$ and $c_\nu = \frac{3-3\nu}{(1+\nu)(1-2\nu)}$. If $\Omega_i$ is not regular enough to provide boundedness of $c_\Omega$, we may employ a suitable cut-off function instead of the $a$-harmonic extensions in $L_{i,\Gamma_{12}}$. Applying Korn's second inequality on the quotient space $\mathcal{H}(\mu)$ with a constant $c_K$ and Lemma 4.1 yields $\|u^0(\mu)|_{\Gamma_{12}}\|_{\Gamma_{12}} \leq (2 + 2c_\Omega c_\nu c_K^2)^{1/2} |||u^0(\mu)|||_\mu$. Choosing $C_2(\Omega, \mu) \geq 1 + (2 + 2c_\Omega c_\nu c_K^2)^{1/2}$ concludes the proof. ∎

### B.3. Proofs of section 5.

*Proof of Corollary* 5.1. The proof can be carried out using the ideas of the proofs of Proposition 3.8 and Theorem 4.4. We just remark that to obtain functions whose restriction to a component pair is in the corresponding quotient space $\mathcal{H}(\mu)$, one has to introduce functions $u_{\mathcal{RB}}^\Gamma(\mu) := \arg\inf_{v\in\mathcal{RB}} \|\tilde{u}^0(\mu) - v\|_{[H^1(\Omega_\Gamma)]^3}$ and choose the coefficients of the $a$-harmonic extensions of the rigid body modes of the spectral approximation such that their traces match $u_{\mathcal{RB}}^\Gamma(\mu)|_\Gamma$ on each port, respectively. Here, $\tilde{u}^0(\mu)$ solves (B.20) for the global system. Finally, the constant $\tilde{C}_{\Gamma,1}(\Omega_\Gamma, \mu)$ depends only on the configuration of the component pair thanks to Korn's second inequality. ∎

*Proof of Corollary* 5.2. Again, the statement can be proved using the same ideas as in the proofs of Proposition 3.8 and Theorem 4.4. To show boundedness of the term $\sum_{\Gamma\in\Pi} \|\chi_\Gamma^f(\mu)\|_\Gamma / |||u^f(\mu)|||_\mu$ appearing in the estimate which corresponds to (B.19), one may introduce the functions $u_{\mathcal{RB}}^{f,\Gamma}(\mu) := \inf_{v\in\mathcal{RB}} \|u^f(\mu) - v\|_{[H^1(\Omega_\Gamma)]^3}$. Here, $u^f(\mu)$ solves (B.20) for the global system. Note that, thanks to $u^f(\mu)|_\Gamma = \chi_\Gamma^f(\mu)$ and the

orthogonality of $\chi_\Gamma^f(\mu)$ and the functions $\{\chi_{\Gamma,1},\ldots,\chi_{\Gamma,6}\}$ with respect to the $(\cdot,\cdot)_\Gamma$-inner product, we have $\|\chi^f(\mu)\|_\Gamma \le \|(u^f(\mu)-u^{f,\Gamma}_{\mathcal{RB}}(\mu))|_\Gamma\|_\Gamma$ on all ports that do not lie on the boundary of $\Omega$. The boundedness of $\sum_{\Gamma\in\Pi}\|\chi_\Gamma^f(\mu)\|_\Gamma/|||u^f(\mu)|||_\mu$ by a constant that only depends on the configuration of the component pair then follows from Korn's inequality. ∎

**Acknowledgments.** We would like to thank Dr. D. J. Knezevic of Akselos for the development of the scRBE library code and Dr. D. B. P. Huynh of Akselos for the graphical user interface software for assembling models. We are grateful to the company Akselos for sharing their I-beam component meshes. Finally, we would also like to thank A. Buhr from the University of Münster for making us aware of a problematic formulation in the spectral greedy algorithm in an earlier version of this paper.

## REFERENCES

[1] A. Abdulle and P. Henning, *A reduced basis localized orthogonal decomposition*, J. Comput. Phys., 295 (2015), pp. 379–401.

[2] I. Babuška, X. Huang, and R. Lipton, *Machine computation using the exponentially convergent multiscale spectral generalized finite element method*, ESAIM Math. Model. Numer. Anal., 48 (2014), pp. 493–515.

[3] I. Babuška and R. Lipton, *Optimal local approximation spaces for generalized finite element methods with application to multiscale problems*, Multiscale Model. Simul., 9 (2011), pp. 373–406, doi:10.1137/100791051.

[4] M. Bampton and R. Craig, *Coupling of substructures for dynamic analyses*, AIAA J., 6 (1968), pp. 1313–1319.

[5] P. Binev, A. Cohen, W. Dahmen, R. DeVore, G. Petrova, and P. Wojtaszczyk, *Convergence rates for greedy algorithms in reduced basis methods*, SIAM J. Math. Anal., 43 (2011), pp. 1457–1472, doi:10.1137/100795772.

[6] F. Bourquin, *Component mode synthesis and eigenvalues of second order operators: Discretization and algorithm*, RAIRO Modél. Math. Anal. Numér., 26 (1992), pp. 385–423.

[7] A. Buffa, Y. Maday, A. T. Patera, C. Prud'homme, and G. Turinici, *A priori convergence of the greedy algorithm for the parametrized reduced basis method*, ESAIM Math. Model. Numer. Anal., 46 (2012), pp. 595–603.

[8] M. Dauge, E. Faou, and Z. Yosibash, *Plates and Shells: Asymptotic Expansions and Hierarchic Models*, Encyclopedia Comput. Mech., John Wiley, New York, 2004.

[9] R. DeVore, G. Petrova, and P. Wojtaszczyk, *Greedy algorithms for reduced bases in Banach spaces*, Constr. Approx., 37 (2013), pp. 455–466.

[10] Y. Efendiev, J. Galvis, and T. Y. Hou, *Generalized multiscale finite element methods (GMsFEM)*, J. Comput. Phys., 251 (2013), pp. 116–135.

[11] J. L. Eftang and A. T. Patera, *Port reduction in parametrized component static condensation: Approximation and a posteriori error estimation*, Internat. J. Numer. Methods Engrg., 96 (2013), pp. 269–302.

[12] J. L. Eftang and A. T. Patera, *A port-reduced static condensation reduced basis element method for large component-synthesized structures: Approximation and* a posteriori *error estimation*, Adv. Modeling Simul. Engrg. Sci., 1 (2014), pp. 1–49.

[13] Eigen, *A C++ Linear Algebra Library*, http://eigen.tuxfamily.org/.

[14] B. Haasdonk, *Convergence rates of the POD-greedy method*, ESAIM Math. Model. Numer. Anal., 47 (2013), pp. 859–873.

[15] B. Haasdonk, *Reduced basis methods for parametrized PDEs: A tutorial introduction for stationary and instationary problems*, in Model Reduction and Approximation: Theory and Algorithms, P. Benner, A. Cohen, M. Ohlberger, and K. Willcox, eds., SIAM, Philadelphia, to appear.

[16] B. Haasdonk and M. Ohlberger, *Reduced basis method for finite volume approximations of parametrized linear evolution equations*, M2AN Math. Model. Numer. Anal., 42 (2008), pp. 277–302.

[17] J. S. Hesthaven, G. Rozza, and B. Stamm, *Certified Reduced Basis Methods for Parametrized Partial Differential Equations*, SpringerBriefs in Mathematics, BCAM SpringerBriefs, Springer; BCAM Basque Center for Applied Mathematics, Bilbao, 2016.

[18] U. Hetmaniuk and A. Klawonn, *Error estimates for a two-dimensional special finite element method based on component mode synthesis*, Electron. Trans. Numer. Anal., 41 (2014), pp. 109–132.
[19] U. Hetmaniuk and R. B. Lehoucq, *A special finite element method based on component mode synthesis*, ESAIM Math. Model. Numer. Anal., 44 (2010), pp. 401–420.
[20] P. Holzwarth and P. Eberhard, *Interface reduction for CMS methods and alternative model order reduction*, IFAC-PapersOnLine, 48 (2015), pp. 254–259.
[21] W. C. Hurty, *Dynamic analysis of structural systems using component modes*, AIAA J., 3 (1965), pp. 678–685.
[22] D. B. P. Huynh, D. J. Knezevic, and A. T. Patera, *A static condensation reduced basis element method: Approximation and a posteriori error estimation*, ESAIM Math. Model. Numer. Anal., 47 (2013), pp. 213–251.
[23] D. B. P. Huynh, D. J. Knezevic, and A. T. Patera, *A static condensation reduced basis element method: Complex problems*, Comput. Methods Appl. Mech. Engrg., 259 (2013), pp. 197–216.
[24] L. Iapichino, A. Quarteroni, and G. Rozza, *A reduced basis hybrid method for the coupling of parametrized domains represented by fluidic networks*, Comput. Methods Appl. Mech. Engrg., 221/222 (2012), pp. 63–82.
[25] L. Iapichino, A. Quarteroni, and G. Rozza, *Reduced basis method and domain decomposition for elliptic problems in networks and complex parametrized geometries*, Comput. Math. Appl., 71 (2016), pp. 408–430.
[26] H. Jakobsson, F. Bengzon, and M. G. Larson, *Adaptive component mode synthesis in linear elasticity*, Internat. J. Numer. Methods Engrg., 86 (2011), pp. 829–844.
[27] B. S. Kirk, J. W. Peterson, R. H. Stogner, and G. F. Carey, *libMesh: A C++ library for parallel adaptive mesh refinement/coarsening simulations*, Engineering with Computers, 22 (2006), pp. 237–254.
[28] D. J. Knezevic and J. W. Peterson, *A high-performance parallel implementation of the certified reduced basis method*, Comput. Methods Appl. Mech. Eng., 200 (2011), pp. 1455–1466.
[29] A. Kolmogoroff, *Über die beste Annäherung von Funktionen einer gegebenen Funktionenklasse*, Ann. of Math. (2), 37 (1936), pp. 107–110.
[30] J.-L. Lions and E. Magenes, *Non-homogeneous Boundary Value Problems and Applications* 1, Springer-Verlag, Berlin, 1972.
[31] Y. Maday and E. M. Rønquist, *A reduced-basis element method*, J. Sci. Comput., 17 (2002), pp. 447–459.
[32] Y. Maday and E. M. Rønquist, *The reduced basis element method: Application to a thermal fin problem*, SIAM J. Sci. Comput., 26 (2004), pp. 240–258, doi:10.1137/S1064827502419932.
[33] I. Maier and B. Haasdonk, *A Dirichlet–Neumann reduced basis method for homogeneous domain decomposition problems*, Appl. Numer. Math., 78 (2014), pp. 31–48.
[34] I. Martini, G. Rozza, and B. Haasdonk, *Reduced basis approximation and a-posteriori error estimation for the coupled Stokes-Darcy system*, Adv. Comput. Math., 41 (2015), pp. 1131–1157.
[35] N. C. Nguyen, *A multiscale reduced-basis method for parametrized elliptic partial differential equations with multiple scales*, J. Comput. Phys., 227 (2008), pp. 9807–9822.
[36] E. C. Pestel and F. A. Leckie, *Matrix Methods in Elastomechanics*, McGraw-Hill, New York, 1963.
[37] A. Pinkus, *n-Widths in Approximation Theory*, Ergeb. Math. Grenzgeb. (3) 7, Springer-Verlag, Berlin, 1985.
[38] A. Quarteroni, A. Manzoni, and F. Negri, *Reduced Basis Methods for Partial Differential Equations. An Introduction*, Unitext 92, Springer, Cham, Switzerland, 2016.
[39] A. Quarteroni and A. Valli, *Domain Decomposition Methods for Partial Differential Equations*, reprint, Numerical Mathematics and Scientific Computation, The Clarendon Press, Oxford University Press, New York, 2005.
[40] F. Schindler, B. Haasdonk, S. Kaulmann, and M. Ohlberger, *The localized reduced basis multiscale method*, in Proceedings of Algoritmy 2012, Conference on Scientific Computing, Vysoke Tatry, Podbanske, 2012, Slovak University of Technology in Bratislava, Publishing House of STU, 2012, pp. 393–403.
[41] K. Smetana, *A new certification framework for the port reduced static condensation reduced basis element method*, Comput. Methods Appl. Mech. Engrg., 283 (2015), pp. 352–383.
[42] K. Smetana and A. T. Patera, *Fully localized a posteriori error estimation for the port reduced static condensation reduced basis element method*, in preparation, 2016.

[43] M. S. Troitsky, *Stiffened Plates: Bending, Stability, and Vibrations*, Elsevier Scientific, Amsterdam, 1976.

[44] K. Veroy, C. Prud'homme, D. V. Rovas, and A. T. Patera, *A posteriori error bounds for reduced-basis approximation of parametrized noncoercive and nonlinear elliptic partial differential equations*, in Proceedings of the 16th AIAA Computational Fluid Dynamics Conference, AIAA Paper 2003-3847, 2003.

[45] W. Weaver, Jr., S. P. Timoshenko, and D. H. Young, *Vibration Problems in Engineering*, John Wiley & Sons, New York, 1990.